FLAME 1.0: a novel approach for modelling burned area in the Brazilian biomes using the Maximum Entropy concept

Maria Lucia Ferreira Barbosa[1,2,*], Douglas I Kelley[3], Chantelle A Burton[4], Igor J M Ferreira[1,5], Renata Moura da Veiga[1], Anna Bradley[4], Paulo Guilherme Molin[2], Liana O Anderson[6]

[1] National Institute for Space Research - INPE, Avenida dos Astronautas, 1758. Jd. Granja - São José dos Campos - São Paulo, 12227-010, Brazil

[2] Federal University of São Carlos, Rodovia Lauri Simões de Barros, km 12 - SP-189 - Aracaçu, Buri - São Paulo, 18290-000, Brazil

[3] UK Centre for Ecology and Hydrology, Wallingford. OX10 8BB UK

[4] Met Office Hadley Centre, Fitzroy Road, Exeter. EX1 3PB UK

[5] Faculty of Environment, Science and Economy, University of Exeter, Exeter, UK

[6] National Centre for Monitoring and Early Warning of Natural Disasters - Cemaden, Estrada Doutor Altino Bondensan, 500 - Distrito de Eugênio de Melo, São José dos Campos - São Paulo, Brazil

* Correspondence to: Maria Lucia Ferreira Barbosa (malucsp@gmail.com)

Abstract

As fire seasons in Brazil lengthen and intensify, the need to enhance fire simulations and comprehend fire drivers becomes crucial. Yet determining what drivers burning in different Brazilian biomes is a major challenge, with the highly uncertain relationship between drivers and fire. Finding ways to acknowledge and quantify that uncertainty is critical in ascertaining the causes of Brazil's changing fire regimes. We propose FLAME (Fire Landscape Analysis using Maximum Entropy), a new fire model that integrates Bayesian inference with the ~~M~~maximum ~~E~~entropy ~~(MaxEnt)~~ concept, enabling probabilistic reasoning and uncertainty quantification. FLAME utilizes bioclimatic, land cover and human driving variables to model fires. We apply FLAME to Brazilian biomes, evaluating its performance against observed data for three categories of fires: all fires (ALL), fires reaching natural vegetation (NAT), and fires in non-natural vegetation (NON). We assessed burned area responses to different explanatory variable groups. The model showed adequate performance for all biomes and fire categories. Maximum temperature and precipitation together are important factors influencing burned area in all biomes. The number of roads and amount of forest boundaries (edge densities), and forest, pasture and carbon in dead vegetation~~soil carbon~~ showed higher uncertainties among the responses. ~~The potential response of these explanatory variables displayed similar spatial likelihood of the observations given the model, between the ALL, NAT and NON categories.~~

39 Overall, the uncertainties were larger for the NON-category, particularly for Pampas and
40 Pantanal regions. Customizing explanatory variable selection and fire categories based on
41 biome characteristics could contribute to a more biome-focused and contextually relevant
42 analysis. Moreover, prioritizing regional-scale analysis is essential for decision-makers and fire
43 management strategies. FLAME is easily adaptable to be used in various locations and periods,
44 serving as a valuable tool for more informed and effective fire prevention measures.
45
46 Keywords: Burned Area. Brazilian biomes. Maximum Entropy. Bayesian Inference. Climate.
47 Fragmentation. Land Use.
48
49
50 **1 INTRODUCTION**
51
52 The complexity of the interactions and feedbacks between fire, climate, people, and other earth
53 system components makes it challenging to be highly confident about what drives fires in
54 specific locations. Various methods assess the drivers of historical fire events. Some studies
55 correlate individual drivers with burned area but overlook the interaction of multiple factors
56 (Andela et al., 2017; Barbosa et al., 2019). Fire Danger Indices capture simultaneous drivers to
57 gauge fire risk. However, they overlook human-driven ignition causes (Zacharakis; and
58 Tsihrintzis, 2023) and typically fail to capture the impact of fuel availability on burning
59 (Kelley; and Harrison, 2014). Fire-enabled ~~Land Surface Models~~Terrestrial Biosphere Models
60 account for these drivers, simulating observable fire regime measures. However, they often
61 lack accuracy for year-to-year fire patterns and required accuracy to determine fire drivers
62 (Forkel et al. 2019) and the causes of individual fire seasons (Hantson et al., 2020). Quantifying
63 uncertainty is critical for assigning fire drivers because it allows for a more accurate assessment
64 of the confidence in our predictions and helps identify the most influential factors under varying
65 conditions. In this sense, research applying the Maximum Entropy framework combined with
66 Bayesian Inference can address these gaps.
67
68 The Principle of Maximum Entropy ~~(MaxEnt)~~ states that when trying to estimate the
69 probability of an event and the information is limited, you should opt for the distribution that
70 preserves the greatest amount of uncertainty (i.e., maximizes entropy) while still adhering to
71 your given constraints (Penfield, 2003). These constraints reflect prior knowledge about the
72 probability distribution of a phenomenon of interest (i.e., burned area) based on its relationship
73 with explanatory ~~independent~~ variables. This approach ensures you do not introduce extra

74 assumptions or biases into your calculations. Max~~imum Ee~~ntropy method has its roots in
75 statistical mechanics (Jaynes, 1957). However, the use of its concept in a species distribution
76 model~~, also~~ called MaxEnt (Phillips et al., 2006)~~,~~ popularized the approach in several other
77 study areas, including ecology, geophysics, and fires (Jin et al., 2020; Li et al., 2019; Fonseca
78 et al., 2017). ~~Incorporating Bayesian Inference alongside the maximum entropy MaxEnt~~
79 ~~framework further enhances this approach. Bayesian techniques integrate prior knowledge and~~
80 ~~observed data to continuously refine the estimation of uncertainty in the influence of drivers~~
81 ~~on fire, thereby improving the confidence in a relationship we find (Kelley et al., 2019). By~~
82 ~~leveraging both maximum entropy MaxEnt and Bayesian Inference, we can develop more~~
83 ~~robust models that account for the complex and dynamic nature of fire regimes.~~

84

85 The MaxEnt species distribution model estimates the probability of target presence for given
86 local conditions (Phillips et al., 2006). Unlike many traditional models, MaxEnt makes minimal
87 assumptions about the relationships between explanatory variables, making it more flexible
88 and adaptable to complex ecological interactions. Rather than estimating a single value,
89 MaxEnt models a full probability distribution (Elith et al., 2011), providing a comprehensive
90 view of potential outcomes. This probabilistic nature enables the incorporation of prior
91 information into the modeling process, enhancing its accuracy. Additionally, MaxEnt enables
92 the quantification of uncertainties (Chen et al., 2019), providing valuable insights into the
93 reliability and confidence of model predictions.

94

95 Recognizing that fires can be treated as a species due to their strong dependence on
96 environmental factors, utilizing the MaxEnt species model has yielded valuable insights into
97 the field (Ferreira et al., 2023; Fonseca et al., 2019). However, the MaxEnt model relies on
98 presence-only or presence/absence data, which means it primarily considers locations where
99 the target (in this case, fires) has occurred. This limits fire research using maximum entropy
100 ~~MaxEnt~~ as it does not allow continuous data, such as burned area fraction over a larger region.
101 Moreover, the constraints and structure of the underlying model are fundamentally related to
102 species distributions (Phillips et al., 2006) rather than fires, which may not capture the nuances
103 of fire behavior.

104

105 Incorporating Bayesian Inference alongside the maximum entropy framework provides a
106 powerful approach. Bayesian techniques integrate prior knowledge and observed data to
107 continuously refine the estimation of uncertainty in the influence of drivers on fire, thereby

improving the confidence in a relationship we find (Kelley et al., 2019). By leveraging both maximum entropy and Bayesian Inference, we can develop more robust models that account for the complex and dynamic nature of fire regimes.

The simulation of fires in heterogeneous territories such as Brazil is incredibly challenging. Wildfires have become a pressing concern in the country, causing significant socioeconomic and environmental losses (Campanharo et al., 2019; Barbosa et al., 2022; Wu et al., 2023). Since Between 1985 and 20220, more than 1,857,025 km² of Brazil's terrain has burned at least once been negatively impacted by fires (MapBbiomas, 2023)., reflecting a need for effective and adaptive fire management strategies. While some ecosystems, such as grasslands and savannas, depend on periodic fires to sustain their biodiversity and ecological processes, the increasing fire frequency driven by agricultural and ranching activities has impacted all Brazilian ecosystems, making them significant terrestrial carbon sources (Cano-Crespo et al, 2023[IF1]). In fire-adapted ecosystems like savannas, disruptions to fire regimes - whether through suppression or excessive frequency - can alter ecological balance, severely damaging fauna, hindering seedling development, and increasing tree mortality. High-intensity and long-duration fires further exacerbate these effects, demonstrating the fine balance required to maintain ecosystem structure and composition (Alvarado [IF2]et al., 2020).Nonetheless, q Quantifying the influence of these drivers, however, can beremains difficult, as many interactions between fire and its drivers are non-linear, and drivers heavily interdependent.act with each other, making This complexity makes confidently identifying drivers of fire regimes in such diverse landscapes challenging tricky from observations alone (Krawchuk and Moritz 2014). While traditional fire models provide useful broadscale information on fire, land, and climate interactions, they often lack the ability to do not quantify the uncertainty in these relationships and rely on other studies to infer relationships between drivers and burning (Hantson et al., 2016).

Improving fire simulations and understanding the underlying drivers of fires in Brazil is essential to address the challenges associated with preventing fires, firefighting, and managing their aftermath. Here, we present and evaluate a novel fire model, FLAME (Fire Landscape Analysis using Maximum Entropy), based on a Bayesian inference implementation of the maximum entropy MaxEnt concept. This combination allows us to incorporate uncertainty and probabilistic reasoning into fire modeling. In this sense, the model aims to precisely measure

141 uncertainties of the simulations. The model optimizes key driving variables relationship with

142 fires. Here we apply FLAME to the biomes in Brazil, and assess the performance against

143 observations.

144

2 METHODS

146

2.1 Brazilian biomes

148

Our study focuses on Brazil, with the Brazilian biomes serving as the primary units of analysis. Brazil comprises six official major biomes, whose boundaries are defined by the National Institute of Geography and Statistics (IBGE; https://www.ibge.gov.br/apps/biomas/#/home), are they: Amazonia, Atlantic Forest, Cerrado, Pampa and Pantanal. This categorization follows Hardesty et al. (2005), which defines biomes based on the predominant vegetation type. However, the six biomes contain vegetation types with different sensitivities to fire. In general, Amazonia and Atlantic Forest are fire-sensitive biomes (Fig. 1) that are highly susceptible to damage or destruction by fire. Conversely, Cerrado, Pampa and Pantanal have evolved to depend on fire as part of their life cycle and are considered fire-dependent biomes. Finally, Caatinga is a fire-independent biome that is generally not significantly affected by fire or does not require fire as part of its vegetation dynamics.

160

161
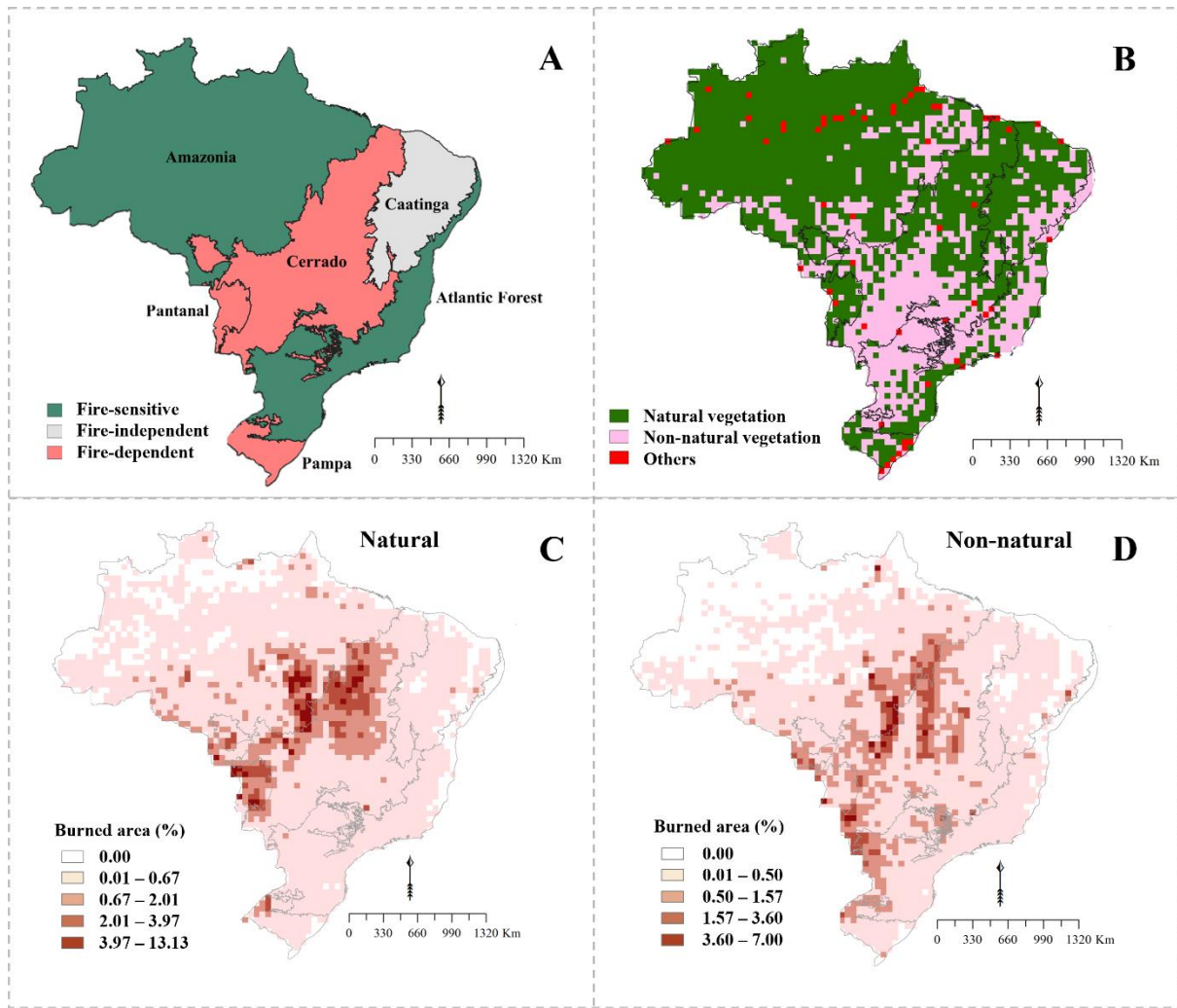
Figure 1: (A) Brazilian biomes classified as Fire-sensitive, Fire-independent and Fire-dependent on the left (Hardesty et al. 2005), (B) Natural vegetation (Forests, Grasslands and Savannas) and Non-natural vegetation (Pasture, Cropland and Forest Plantations) in 2019 in Brazil. (C) NAT's mean burned area percentage per pixel and (D) is the NON's mean burned area percentage per pixel. The maps (C and D) show the mean for August, September and October from 2002 to 2019.

2.2~~1~~ Datasets and preprocessing

We used the MCD64A1 burned area product from MODIS collection 6 as our target variable (Giglio et al., 2018). This data was regridded from 500 m to 0.5° spatial resolution by dividing the total burned area within each coarse cell by its total area. The burned area data was used in its totality (ALL) and divided into two other categories based on the Land Use and Land Cover (LULC) data from the MapBiomas~~Mapbiomas~~ project (https://brasil.mapbiomas.org/en/): ~~fires~~

reaching burned areas in natural vegetation (NAT) and ~~fires reaching~~ burned areas in non-natural vegetation (NON) (Fig. 1).We computed all burned areas within forests, grasslands, and savannas for the NAT and ~~the NON~~ within pasture, cropland, and forest plantation~~,~~ (aggregated with croplands) for the NON category. The categorization of fires aims to assess whether there are distinct drivers for NAT and NON and to exemplify the potentialities of the model for assessing more than one fire category across different vegetation types. We adopt a broad approach to encompass the various biomes in Brazil; however, any type of categorization is permissible, and further studies could focus on even finer stratification, e.g., fires affecting fire-sensitive vegetation and fire-dependent vegetation within each biome.

~~Hardesty et al. (2005), which defines biomes based on the predominant vegetation type. However, all biomes contain vegetation types with different sensitivities to fire, Amazonia and Atlantic Forest are fire sensitive biomes (Fig. 1) that are highly susceptible to damage or destruction by fire. Conversely, Cerrado, Pampa and Pantanal have evolved to depend on fire as part of their life cycle and are considered fire-dependent biomes. Finally, Caatinga is a fire-independent biome that is generally not significantly affected by fire or does not require fire as part of its vegetation dynamics. This categorization follows Hardesty et al. (2005), based on the predominant vegetation type that defines the biome. However, all biomes contain vegetation types with different sensitivities to fire. We adopt a broad approach to encompass the various biomes in Brazil; however, any type of categorization is permissible, and further studies could focus on even finer stratification, e.g., fires reaching affecting fire sensitive vegetation and fire-dependent vegetation within each biome.~~

The target and explanatory ~~independent~~ variables were extracted for August, September, and October, from 2002 to 2019, representing the general peak of the fire season in Brazil. This time frame is the most extended overlapping period between the datasets which we further divided into a training phase from 2002 to 2009 and a validation phase from 2010 to 2019. The explanatory ~~independent~~ variables were divided into five groups (climate, anthropogenic and natural ignition, fuel, LULC and forest metrics) and are described in Table 1.

We acquired monthly climate explanatory variables from the first component of the third simulation round of the Inter-Sectoral Impact Model Intercomparison Project (ISIMIP3a, https://www.isimip.org/). ISIMIP is a collaborative effort to compare and evaluate the outputs of various climate and impact models (Frieler et al., 2023). This data represents the historical simulations using climate-forcings from GSWP3-W5E5, available from 1901 to 2019 at a 0.5° spatial resolution. The explanatory variable consecutive dry days tracks the continuous count of dry days since the last recorded rainfall, beginning in the 1900s. The monthly maximum of this ongoing value is then calculated.

We obtained carbon in dead vegetationsoil, vegetation carbon and soil moisture from the Joint UK Land Environment Simulator Earth System impacts model at version 5.5 (JULES-ES; Mathison et al., 2023) and driven by ISIMIP3a GSWP3-W5E5 as per Frieler et al. (2023), which is freely available at https://www.isimip.org/impactmodels/details/292/. JULES-ES has previously been used as input for Bayesian-based fire models (e.g. UNEP et al., 2022). JULES dynamically models vegetation, carbon fluxes and stores in response to meteorology, hydrology, nitrogen availability, and land use change. JULES-ES has been extensively evaluated against snapshots and site-based measurements of vegetation cover and carbon (Mathison et al., 2023; Wiltshire et al. 2021; Burton et al., 2019; Burton et al. 2022). As per UNEP et al. (2022), vegetation responses to JULES-ES's internal fire model were turned off so as not to double-count the effects of burning. The maps, therefore, represent environmental carbon potential and are applicable to FLAME as the model only assumes that explanatory variable ranges are correctly ranked – i.e. areas of low/high carbon content correspond with real-world areas of low/high carbon and not that the absolute magnitude is correct.

Regarding ignition explanatory variables, Population Density data was also obtained from the ISIMIP3a protocol and based on data from the History Database of the Global Environment (HYDE) v3.3 (Volkholz et al., 2022). Lightning was prescribed as a monthly climatology from LIS/OTD data (CECIL, 2006). The LIS/OTD Climatology datasets comprise gridded climatologies that document the lightning flash rates detected by the Optical Transient Detector (OTD) and the Lightning Imaging Sensor (LIS) aboard the Tropical Rainfall Measuring Mission (TRMM). We collected rTotal road density (in m/km²) data from the Global Roads Inventory Project (GRIP) (MEIJER et al. 2018), was calculated for each grid cell of 0.5-degree of spatial resolution using linear interpolation in the Iris Python package (MET OFFICE, 2023), based on road density data from the Global Roads Inventory Project (GRIP) (MEIJER et al.

246 2018).total density in m/km², which we regridded to the 0.5-degree grid used by the rest of the

247 data using linear interpolation in the Iris Python package (MET OFFICE, 2023).

249 We used the collection 7 LULC data from the MapBiomas project, which produces annual

250 LULC mapping for the Brazilian territory. They were regridded from 30 m to 0.5∘ to match

251 the coarser resolution and linearly interpolated from an annual to a monthly time step.

253 We incorporated forestthese metrics to integrate fragmentation explanatory variables.

254 Sstudies suggest that these are linked to fire occurrence in Amazonia and Cerrado (Silva Junior

255 et al., 2022; Rosan et al., 2022) but remain unexplored in the other biomes. The forest metrics

256 variables were also calculated into the 0.5° grid based on the annual forest data from the

257 MapBiomasMapbiomas at 30m resolution using the package 'landscapemetrics' available in R

258 (Hesselbarth et al., 2023). The metrics were number of forest patches (NP) and forest edge

259 density (ED), described below:.

$$NP = n_i \tag{1}$$

262 where n_i is the number of patches belonging to class i. NP is an 'Aggregation metric' and

263 describes the fragmentation of a class, in this case, forest formations.

$$ED = \frac{\sum ee_i}{A} \tag{12}$$

266 where ee_i is the total forest edge length in meters, and A is the total landscape area in square

267 meters. It quantifies edge density per pixel by summing up all forest edges within class i in

268 relation to the overall landscape area. We incorporated these metrics to integrate fragmentation

269 explanatory variables - studies suggest that these are linked to fire occurrence in Amazonia and

270 Cerrado (Silva Junior et al., 2022; Rosan et al., 2022) but remain unexplored in the other

271 biomes.

Group	Explanatory Variable	Temporal availability	Selected (Yes/No)	Abbreviation	Source
CLIMATE	Maximum Temperature (ºC)	Monthly	Yes	tmax	ISIMIP3a Frieler et al. (2023)
	Precipitation (m/sec)	Monthly	Yes	ppt	
	Vapor pressure deficit (Pa)	Monthly	No	vpd	
	Relative Humidity (fraction)	Monthly	No	rh	
	Consecutive number of dry days (days)	Monthly	No	dry_days	
	Soil Moisture (fraction)	Monthly	No	soilM	JULES-ES
	Population density (people/1000 km^2)	Annual	No	pop	ISIMIP3a Frieler et al. (2023)
	Road density (m/m^2)	Constant	Yes	road	GRIP global (Meijer et al., 2018)
FUEL	Vegetation carbon (kg/m2)	Monthly	No	cveg	JULES-ES
	Soil carbonCarbon in dead vegetation (kg/m2)	Monthly	Yes	csoil	JULES-ES
LULC	Forest (%)	Annual	Yes	forest	MapBbiomas, 2022
	Grassland (%)	Annual	No	grass	
	Savanna (%)	Annual	No	sav	
	Cropland (%)	Annual	No	crop	

	Pasture (%)	Annual	Yes	pas	
FOREST METRICS	Number of patches	Annual	No	np	Calculated from MapBbiomas, 2022
	Edge density (m/m²)	Annual	Yes	ed	

274   Table 1. ~~Initial l~~List of explanatory variables prior to the removal process as described

275   in Section 2.2.

276 **2.3~~2~~ Explanatory V~~v~~ariables selection**

277

278 In constructing our predictive model, we considered the interrelationships among different

279 explanatory variables to ensure a robust and coherent analysis. The selection of these variables

280 was guided by their correlation, aiming for a set of features that provided information without

281 redundancy. For this, we calculated the Spearman correlation coefficient (Spearman, 1961)

282 presented in Fig. ~~4 .~~2. We chose Spearman rank over other correlation metrics as it is expected

283 ~~our model has a~~ non-linear relationship~~s~~ between the drivers ~~and fires~~ (Section 2.4~~3~~), making

284 it a better assessment than parametric comparisons. We identified explanatory variables ~~that~~

285 ~~exhibited~~with strong relationships by using the Spearman's~~examining the~~ correlation matrix~~,~~

286 ~~which we~~ and removed one variable from each highly correlated pair ~~the final model. We used~~

287 ~~a~~ (threshold higher than 0.6~~) from Spearman's coefficient for this~~. The choice of which variable

288 to remove was informed by ~~selection was also based on~~ previous knowledge ~~about the~~

289 ~~variables~~of their relationship with burned area~~s~~ and their relevance to our study. ~~For example,~~

290 ~~we did not include~~although lightning ~~even though it presented low correlation with other~~

291 ~~explanatory variables, it was excluded because. F~~fires caused by lightning ~~are uncommon and~~

292 ~~typically~~ usually occur during the wet season (Menezes et al., 2022)~~, which is outside of~~the

293 ~~scope of our analysis.~~

294

295

296
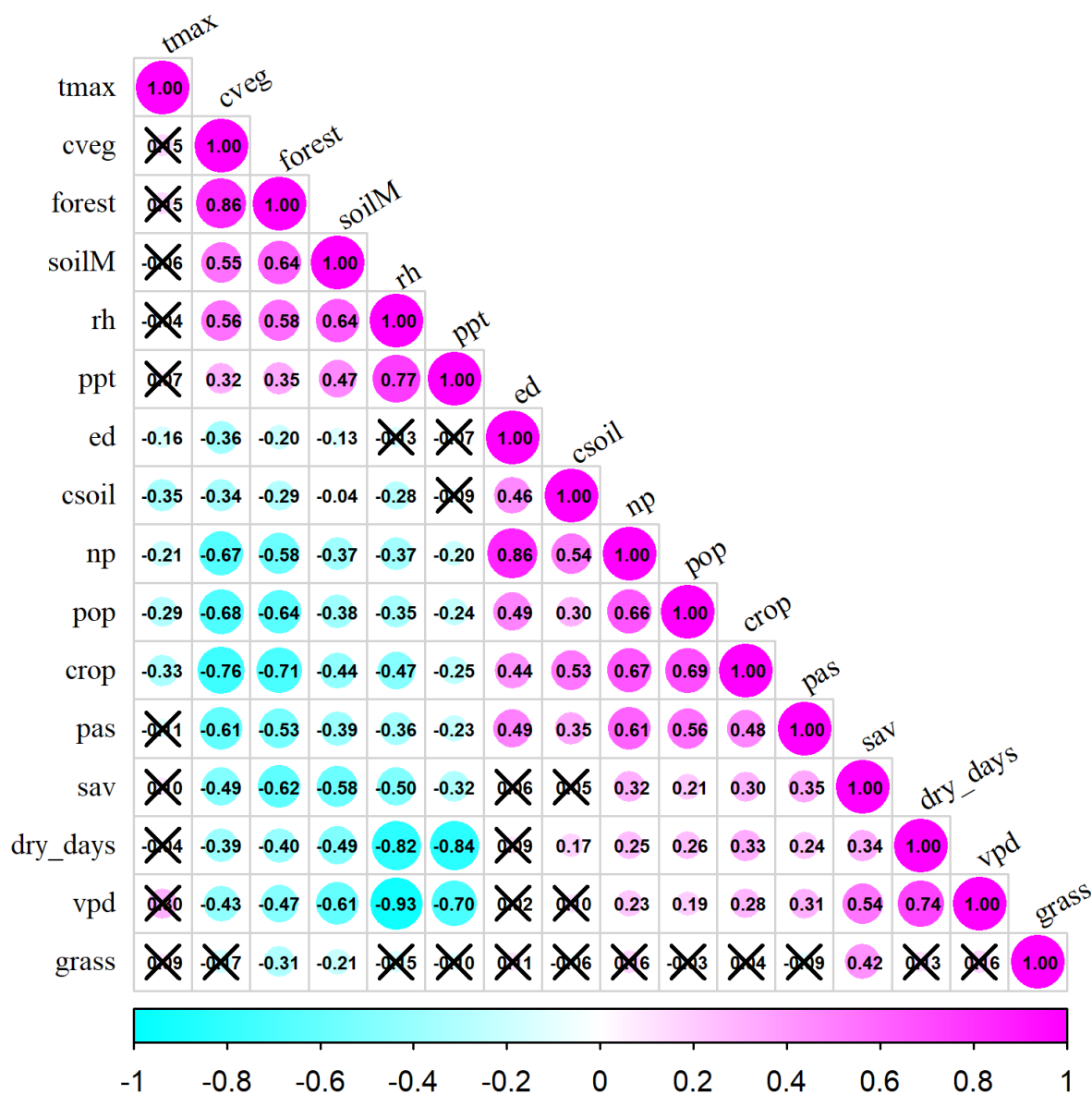
Figure 2: Spearman correlation of the explanatory variables (also see Table 1). Crossed values indicate no correlation, values near 1 [magenta] indicate a strong positive correlation and near -1 [cyan] a strong negative correlation.

We adopted a more streamlined approach by opting for a shorter list of explanatory variables and by grouping them in the variables analysis to capture their compound effect. ~~Initially~~At this stage, we selected 7 explanatory variables as input for the final model (Fig. 3) from the 18 initial explanatory variables. These variables were chosen based on their correlation, ensuring that at least one explanatory variable from each group was selected (Climate, Fuel, LULC, Ignition and Forest Metrics). ~~Next, we divided t~~The explanatory variables were then divided into three groups~~:~~. Group 1 is composed of ~~the climate variables~~ Maximum Temperature and Precipitation which are related with fire weather; Group 2 includes ~~the variables~~ Edge Density

309 and Road Density which are related with landscape fragmentation; and Group 3 encompasses
310 Forest cover, Pasture cover and Carbon in dead vegetation which are associated with fuel
311 availability.

312
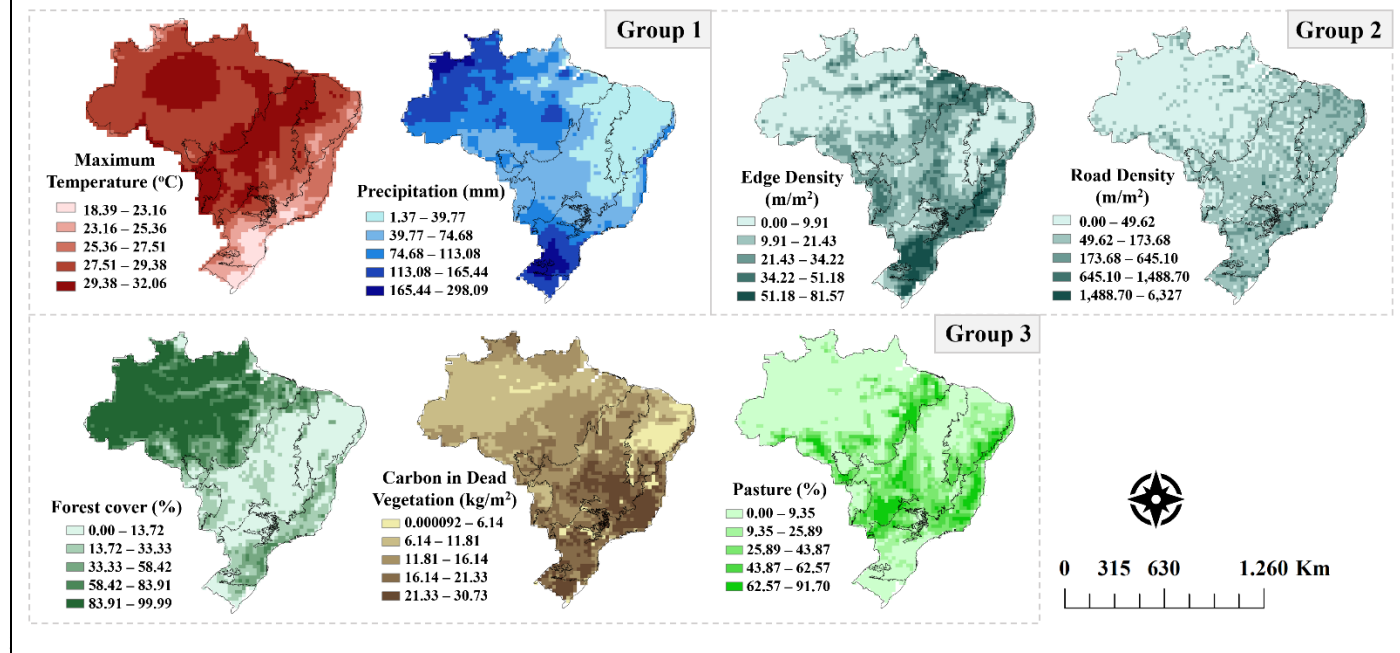
314 **Figure 3: Mean of the selected explanatory variables for August, September and October**
315 **from 2002 to 2019.**

316

317 **2.43 Relationship curves**

318

319 The constraints or priors of the model were added as parameters of different functions, which
320 we refer to as relationship curves. We included the linear and power functions (Fig. 4)
321 according to known relationships between fires and environmental variables. This means that
322 some environmental explanatory variables, when presenting higher values, are likely to
323 increase fires. In comparison, others have an inverse relationship where lower values of the
324 explanatory variable coincide with an increase in burned area. In addition, we added the linear
325 and power functions without imposing a priori constraints on parameters to enforce positive or
326 negative relationships. We expect our selected explanatory variables to have the following
327 relationship with fires:

328   1. Maximum Temperature, Carbon in dead vegetation and Pasture are expected to increase
329   fire activity as their values increase burning with the increase of the variable (Cano-
330   Crespo et al., 2015; Dos Santos et al., 2021; Libonati et al., 2022);

331   2. Precipitation and Forest, which we are expect to increase burning fire activity as their
332   valueswith the decrease of the variable (Aragão et al., 2008; Barbosa et al., 2022);

333   3. Edge Density and Roads are expected to have more uncertain response across the
334   biomes. High density of edges can lead to more fires into forest ecosystems
335   (Armenteras et al., 2013; Silva-Junior et al., 2022) but fragmentation can also reduce
336   fires by impeding fire spread (Driscoll et al., 2021). Regarding Road Density, while
337   more fires are expected surrounding roads (Armenteras et al., 2017), less fires are
338   expected with increased density due to urbanization.

340   The model then estimates the contribution of each curve to the final model. Even though it is
341   possible to include more relationship curves, we decided to keep it at a minimum to avoid
342   making too many assumptions and unstable results due to computational efficiency.
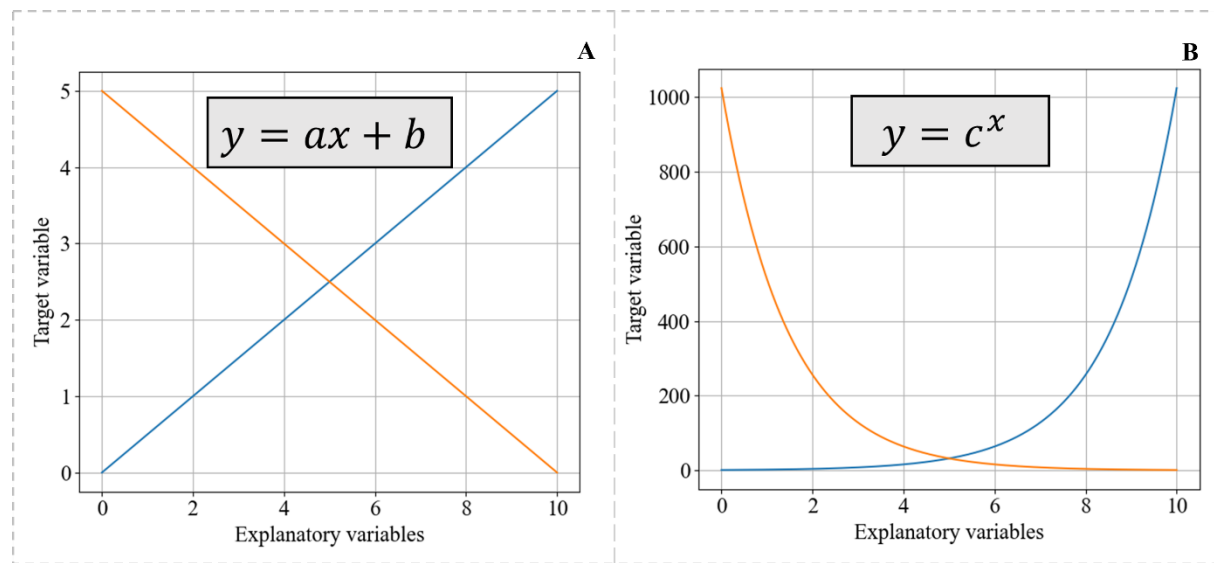
Figure 4: Graphical representation of the relationship functions implemented in the model. (A) ~~The one on the left is a~~ **is a linear function and (B)**~~on the right~~ **is a power function.**

2.~~4~~5 Model optimization

The model was optimized for each Brazilian biome separately using the MCD64A1 product
from 2002 to 2009. This process used the PyMC5 Python package (ABRIL-PLA et al., 2023),
employing 5 chains each over 1000 iterations using the No-U-Turns Hamilton Monte Carlo
sampler (Hoffman and Gelman 2014) while utilizing 20% of the data or a minimum of 6000
grid cells. While the runs were conducted individually for each Biome, the results were

357 aggregated to facilitate visualization. The code used to develop this model is available on

358 Zenodo (Barbosa et al., 2024a)~~GitHub repository~~ (~~https://github.com/malu-barbosa/FLAME~~).

359

360 In Bayesian inference, we update our beliefs or knowledge about a system or event by

361 incorporating new evidence or data (Laplace, 1820; Gelman et al., 2013). It allows us to

362 quantify and update our uncertainty using probability distributions. By maximizing entropy,

363 we aim to achieve the most unbiased, information-rich distribution that satisfies this prior

364 knowledge. In this sense, the likelihood (or posterior probability) of the values of the set of

365 parameters, β, given a series of observations Obs_i and explanatory variables (X_{iv}, from section

366 2.3~~2~~) is proportional ($\propto$) to the prior probability distribution of $P(\beta)$ multiplied by the

367 probability of the observations given the parameters tested.

368

$$P(\beta \,|\, \{Obs_i\}, \{X_{iv}\}) \ \propto \ P(\beta) \ \times \Pi_i \, P(Obs_i | \{X_{iv}\}, \beta) \tag{2\underline{2}3}$$

370

371 Where $\{Obs_i\}$ is a set of our target observations, and i is the individual data point and $\{X_{i\,v}\}$ is

372 the set of explanatory variables, v, for data point i. The pi notation (Π) indicates repeated

373 multiplication. Maximum Entropy in species distribution modeling assumes that individual

374 observations (Obs_i) are either 1 when there is a fire or 0 when there is not, and that:

375 $\qquad P(1 | \{X_v\}, \beta) \ = \ f(\{X_v\}, \beta) \text{ and } \ P(0 | \{X_v\}, \beta) \ = \ 1 - f(\{X_v\}, \beta)$

376 (3\underline{3}4)

377 Where $P(1 | X, \beta)$ is the probability of a fire to occur, $P(0 | X, \beta)$ is the probability of no fire.

378 The term $f(X, \beta)$ is defined below:

$$f(\{X_v\}, \beta) \ = \ 1/(1 + e)^{-y(\{X_v\}, \beta)} \tag{4\underline{4}5}$$

380 where $y(\{X_v\}, \beta)$ = linear function + power function (section 2.4\underline{4}3):

$$y(\{X_v\}, \beta) \ = \ \beta_0 + \Sigma_v (b_{0,i} \times X_v \ + b_{1,v} \, c^{X_v}) \tag{5\underline{5}6}$$

382

383 This works for single land points, where a location burns or does not burn. We extend this

384 concept to derive the Maximum Entropy solution for fractional burned area by integrating over

385 a larger grid cell area. Here we consider that when dividing a grid cell indefinitely, the subcell

sizes approach infinitesimally small values and the data within each subcell starts to behave like continuous data. We adapted Eq. (2~~3~~) and (3~~4~~) to work with continuous data:

$$P(\beta \mid \{Obs_i\}, \{X_{iv}\}) \propto P(\beta) \times \Pi_i^n \Pi_j^s P(Obs_{ij} \mid \{X_{iv}\}, \beta)^{1/s} \tag{6~~7~~}$$

Where n is the observations sample size, j is the individual subgrid, and s is the subgrid sample size. If, for a given Obs_i, m of the s subgrid cells burn, then we can adapt Eq. (3~~4~~) to get:

$$P(m/s \mid \{X_{iv}\}, \beta) = \Pi_j^s P(1 \mid \{X_{iv}\}, \beta)^m \times P(0 \mid \beta)^{s-m}$$

$$= f(\{X_{iv}\}, \beta)^m \times (1 - f(\{X_{iv}\}, \beta))^{~~m~~-s-m} \tag{7~~8~~}$$

and therefore:

$$P(\beta \mid \{m_i/s_i\}, \{X_{iv}\}) \propto P(\beta) \times \Pi_i^n f(\{X_{iv}\}, \beta)^{m/s} \times (1 - f(\{X_{iv}\}, \beta))^{(m-s-m)/s}$$

$$\tag{8~~9~~}$$

When $s \to \infty$, m/s becomes burned area fraction (BF). Then:

$$P(\beta \mid \{BF_i\}, \{X_{iv}\}) \propto P(\beta) \times \Pi_i^n f(\{X_{iv}\}, \beta)^{BF_i} \times (1 - f(\{X_{iv}\}, \beta))^{1-BF_i}$$

$$\tag{9~~10~~}$$

This solution assumes that burning conditions at a specific location solely explain the likelihood of burning. In reality, fires spread and, particularly at higher burned areas, they may overlap. We, therefore, modify Obs_i so that it represents what the burned fraction of a gridcell would looks like if it was one large fire with no overlapping burning:

$$Obs_i = Obs_{i,0} \times (1 + Q) / (Obs_{i,0} \times Q + 1) \tag{10~~11~~}$$

Where $Obs_{i,0}$ is the true observation, and Q is a modifier parameter to remove the effects of fire overlap.

Lastly, to account for variations in land cover to assign between natural and non-natural vegetation, which can be very small in some cells, we introduced a weighting factor w when assessing fire categories. This weighting factor considers the individual area of each grid cell, ensuring that cells with smaller vegetation cover contribute proportionally to the analysis, as in Eq. 1~~1~~2 below:

$$P(\beta \,|\, \{BF\}, \{X_{iv}\}) \propto P(\beta) \times \Pi_i^n f(\{X_{iv}\}, \beta)^{BF_i \times w} \times (1 - f(\{X_{iv}\}, \beta))^{(1-BF) \times w} \quad (1\underline{1}\underline{2})$$

We use weak, uninformed prior distributions for our Eq. ($5\underline{6}$) parameters. β_0, $b_{0,i}$ and $b_{1,i}$ priors were set as a normal distribution with a mean of 0 and a standard deviation of 100, and c a lognormal with a μ of 0 and a σ of 1. The parameter Q in Eq.(10) was set as a log-normal distribution with a μ of 2 and a σ of 1.

2.$\underline{6}\underline{5}$ Model evaluation

The model's main goal is to accurately quantify uncertainties, which we tested by analyzing where the observations fell in the model's posterior probability distribution (Eq. $9\underline{10}$). The uncertainties refer to the difference between the 10th and 90th percentiles of the simulated burned area distribution and provides an estimate of the variability within the model outputs (Fig.5). If more than 20% of the observations fall outside the 10th-90th percentile range, the uncertainty range is too narrow because it fails to encompass the 10th–90th percentile range. Conversely, if observations cluster around the middle of the distribution (50th percentile%), the uncertainty range is too wide as it overestimates the spread of the data. We aim to minimize uncertainty constraints without compromising accuracy. When evaluating the model against 2010-2019 observations, we also investigated how likely the observations are given the optimized model (P(Observed|Simulated)), as per Kelley et al. (2021). Using a different time period from the optimization (from 2002 to 2009), we ensure an independent model evaluation. If the out-of-sample observations are more likely given the model, then the model performs well. We use a likelihood of 50% to indicate adequate performance.

We calculate the probability of an observation given our model (Fig.6) by integrating the observation's likelihood across parameter space, weighted by the parameter likelihood given our training in section 2.$\underline{5}\underline{4}$:

$$P(Y \,|\, (X, \beta \,|\, \{BF_0\}, \{X_0\})) = \int_\beta P(\beta \,|\, \{BF_i\}) \times P(Y|\beta) \, d\beta$$

(1$\underline{2}\underline{3}$)

which, combined with Eq. ($9\underline{10}$), gives us:

$$P(Y \,|\, (X, \beta \,|\, \{BF_0\}, \{X_0\})) = \int_\beta P(\beta \,|\, \{BF_i\}) \times f(X, \beta)^Y \times (1 - f(X, \beta))^{1-Y}$$

(1$\underline{3}\underline{4}$)

Where Y is an observation and X corresponds to the model inputs at the time and location of Y. We approximate this by sampling 200 parameter ensemble members from each of our five chains, providing us with 1000 ensemble members. The frequency of these 1000 in parameter gives us "$P(\beta|\{BF_i\})$" in Eq. (134). We then drive the model with each parameter combination to give us $f(X, \beta)$. We used the iris package (Met Office, 2023) with Python version 3 (Python Software Foundation, https://www.python.org/) for sampling.

We also determined the percentile of our observations within the model's posterior probability distribution. In an unbiased model, we expect the observation position to be essentially random, with the mean over many samples tending towards the middle of the distribution (i.e., a percentile of 50%). We mapped out the mean bias position of the observations for the 30 time steps (3 months, August, September, October, for 10 years) tested (Fig. 76). The p-value in Fig. 87 uses the sStudent t-test to ascertain if the mean of the posterior position of the monthly observations for a given gridcell (mean bias) is significantly different 50% (i.e, the model is biased). A mean bias near 0 indicates that observations are consistently smaller than the simulations, and near 1 indicates that the observations are greater than the simulations. Low p-numbers indicate where the model is biased towards a probability distribution, which tends to suggest too low or high burning.

2.76 Explanatory Vvariables analysis

We assessed the behavior of the explanatory variables against the burned area simulations by generating response maps for our explanatory variable groups in a similar way to Kelley et al. (2019). In the potential maps, we set each explanatory variable in the group to their median and kept the others at their original values. The median, representing the middle value in a dataset, was chosen because it is less affected by extreme values compared to the mean. The maps were subtracted from the original simulations (control - potential response) to quantify the influence of the target group on the model's response. This approach enables the assessment of burned area response when the explanatory variable deviates from the median and assumes its original values which could be below or above the median depending on these original values. The likelihood agreement maps for the potential response are then the percentage of the modeled distribution that shows an increase in burning in each Biome, or, in other words, how likely it is that the potential response is greater than zero. Values near 100% indicate that the group of

variables is confidently associated with an increase in burning at a specific location. Conversely, values near 0% suggest that the variables are leading to a decrease in burning. For values in the middle range (40% to 60%), the response remains uncertain as it is not possible to confidently determine whether the variables are contributing to an increase or decrease in burning.

We evaluate the sensitivity for each group by measuring the gradient's magnitude across its variables, $U = \{X_u\}$ where X_u represents the exploratory variables within group U. The conventional approach to describe a gradient in multidimensional space involves computing the partial derivative for every dimension. In this case, we perform this calculation for each parameter sample, β, across all variables in the group:

$$\nabla_U f(\{X_v\}, \beta) = \left\{ \frac{\delta f(\{X_v\}, \beta)}{\delta x_i} : x_i \in U \right\} \tag{14}$$

The magnitude of this gradient is the root sum square of these partial derivatives:

$$||\nabla_u f(\{X_v\}, \beta)|| = \sqrt{\sum_{x_i \in U} \left(\frac{\delta f(\{X_v\}, \beta)}{\delta x_i} \right)^2} \tag{15}$$

We approximate this by perturbing the exploratory variables in the group by +/- 0.05

$$||\nabla_u f(\{X_v\}, \beta)|| \sim \sqrt{\sum_{j \in u} \frac{(f(\{x_i + \Delta_i\}) - f(\{x_i - \Delta_i\}))^2}{0.1}} \quad \text{where } \Delta_i = \begin{cases} 0.05 & i = j \\ 0 & otherwise \end{cases} \tag{16}$$

To compute the sensitivity response, we took the difference between a simulation where we subtracted 0.05 and added 0.05 fraction of the training range of the explanatory variable of interest. The goal was to understand how burned area responds to marginal variations in the explanatory variables.

3 RESULTS

We present the results in two sections. The first section focuses on the model's performance in simulating the observations, while the second section delves into the simulation's response to the predictor explanatory variables.

3.1 Model simulations and performance

We performed simulations of burned area across each Brazilian biome and fire category, and the resulting maps are shown in Fig. 5. The three simulation runs (ALL, NAT, and NON) successfully captured uncertainties in all Biomes, with most observations falling within the

513 10th to 90th percentiles of the model (See Fig. S1 and S2). However, the model exhibits

514 variations in uncertainties based on the simulation category. For instance, in Amazonia, a

515 biome characterized by a vast expanse of natural vegetation, uncertainties were smaller in NAT

516 simulations, contrasting with larger uncertainties observed in NON-simulations, especially in

517 areas where observed burned areas are small or zero (Fig. 5). Similarly, the Pantanal displayed

518 lower uncertainties in NAT simulations, with values reaching up to 10%, while NON

519 simulations registered uncertainties up to 20% of burned area. The Atlantic Forest, a biome

520 distinguished by non-natural vegetation, exhibited smaller uncertainties in NON simulations.

521 These findings indicate that the segregation of fire categories (ALL/NAT/NON) substantially

522 impacts the model's response. Conversely, the model struggles to accurately capture large

523 burned areas (> 10%) in central regions of Brazil across all three simulations, mostly where the

524 Cerrado biome is located.

525
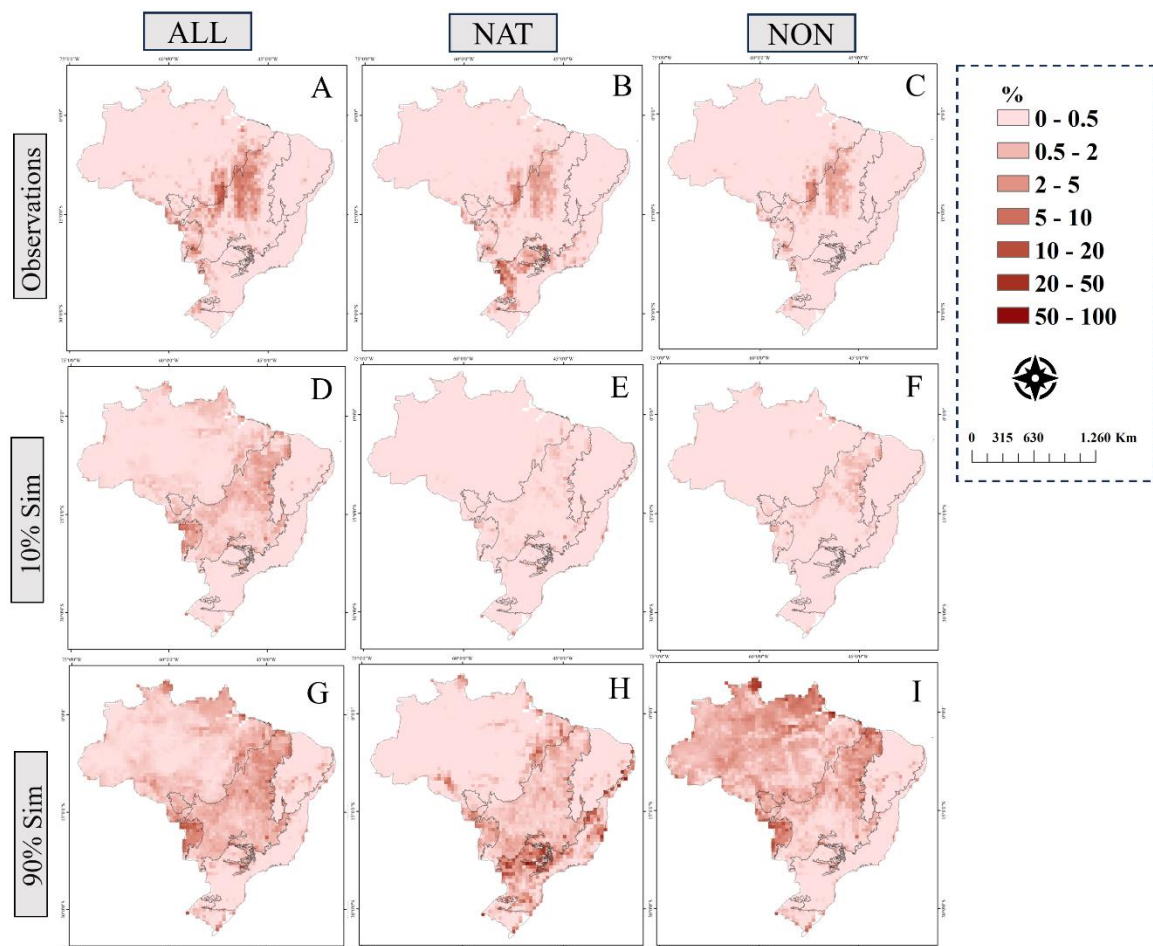
526 **Figure 5: Maps of modeled and observed percentage (%) of burned area. First row: show**
527 **the observed burned area for, July-September 2002-2009 annual average categorized into**
528 **total burned area for (ALL, left)(left), burned area in natural vegetation (NAT, (middle),**
529 **and burned area in non-vegetation (NON, (right). Second and third row show the**

modeled burned areas at the~~: as top row but simulated by the model~~ 10th and 90th percentiles, respectively.

In Bayesian inference, the likelihood expresses the probability of observing a particular event given the model's parameters. Our results imply a strong agreement between the parameters of the model and the observations (Fig. 6~~Table 2~~), even during the months when the observations were less likely. The mean likelihood during these months was above 90% across all Biomes in all simulations, except for the Pantanal, where the likelihood was lower (78% for ALL and 87% for NON) but still satisfactory. The percentiles indicated that in the Pantanal, the likelihood of the observations for ALL varied between 59% to 91%. In contrast, other Biomes presented a minimum likelihood of 80%. During months of best performance, most biomes aligned with the observations, achieving its maximum likelihood (100%) on average. The Pantanal, however, presented the lowest values, with 97% for both ALL and NON simulations.
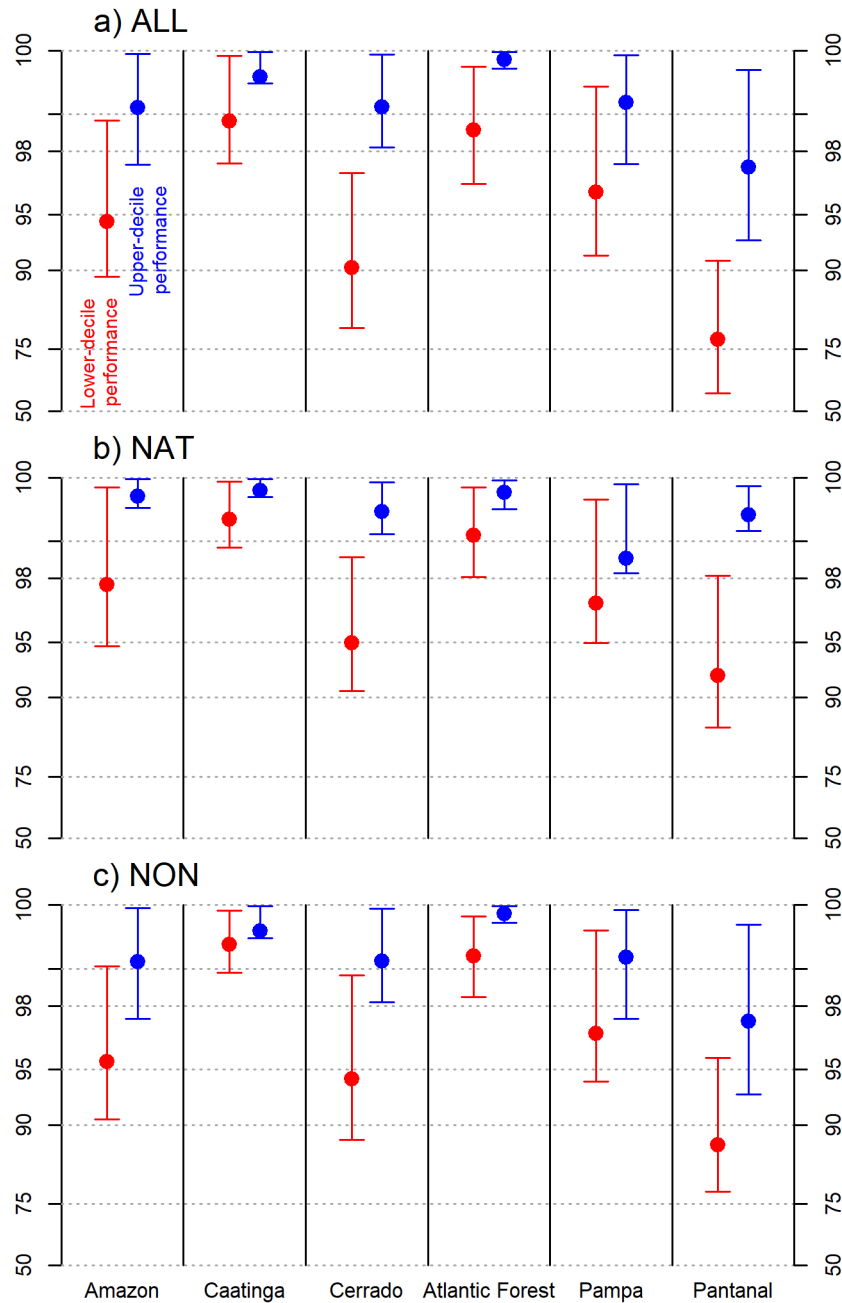
545 **Figure 6: Likelihood (%) per biome of the observations given the model parameters over**
546 **all cells and timesteps. Lower-decline performance is represented in red and Upper-**
547 **decline performance in blue for ALL (a), NAT (b) and NON (c).**

548

549 ~~Table 2. Likelihood (%) per biome of the observations given the model parameters over all~~
550 ~~cells and timesteps. 10% (left) indicates months/cells with worst performance, while 90%~~
551 ~~(right) indicates best performance.~~

	Worst performance			Best performance		
			Likelihood - All fires			
Biome	Mean	10th percentile	90th percentile	Mean	10th Percentile	90th Percentile
Amazon	95	89	99	99	98	100
Caatinga	99	98	100	100	100	100
Cerrado	90	80	97	99	98	100
Atlantic Forest	99	97	100	100	100	100
Pampa	96	92	100	99	98	100
Pantanal	78	59	91	97	93	100
			Natural			
Amazon	98	95	100	100	100	100
Caatinga	99	99	100	100	100	100
Cerrado	95	91	99	100	99	100
Atlantic Forest	99	98	100	100	100	100
Pampa	97	95	100	99	98	100
Pantanal	92	86	98	100	99	100
			Non - natural			
Amazon	95	91	99	99	98	100
Caatinga	99	99	100	100	100	100
Cerrado	94	88	99	99	98	100
Atlantic Forest	99	98	100	100	100	100
Pampa	97	94	100	99	98	100
Pantanal	87	78	96	97	93	100

552

553

554 ~~Figure 6 presents the likelihood per pixel. Areas without values indicate zones where burned~~

555 ~~area is zero, making the likelihood calculations inapplicable.~~ The spatial likelihood analysis

556 (see Fig. S3) provides additional insights into the model's robustness across different biomes

557 and fire categories. The results underscore the model's effective performance across the

558 biomes. Notably, the likelihood remained very high for the Atlantic Forest, Caatinga, and

559 Pampa biomes even in the months and locations where observations were less likely. A high

560 likelihood is also observed for NAT in Amazonia, except for the south and east, which contain

561 most of the non-natural vegetation. Lower performance is evident in the simulations for both

562 ALL and NON in this Biome, indicating that stratifying fire categories by vegetation type is

563 ~~could be~~ a good strategy to enhance model performance in Amazonia. ~~, or isolating fire~~

564 ~~categories where the model has higher predictive ability~~. Similarly, the Pantanal showed the

565 best performance for NAT, but lower performance for ALL and NAT across the majority of

566 the Biome. In contrast, Cerrado performed better than most biomes for NON during the months

567 of worst performance.
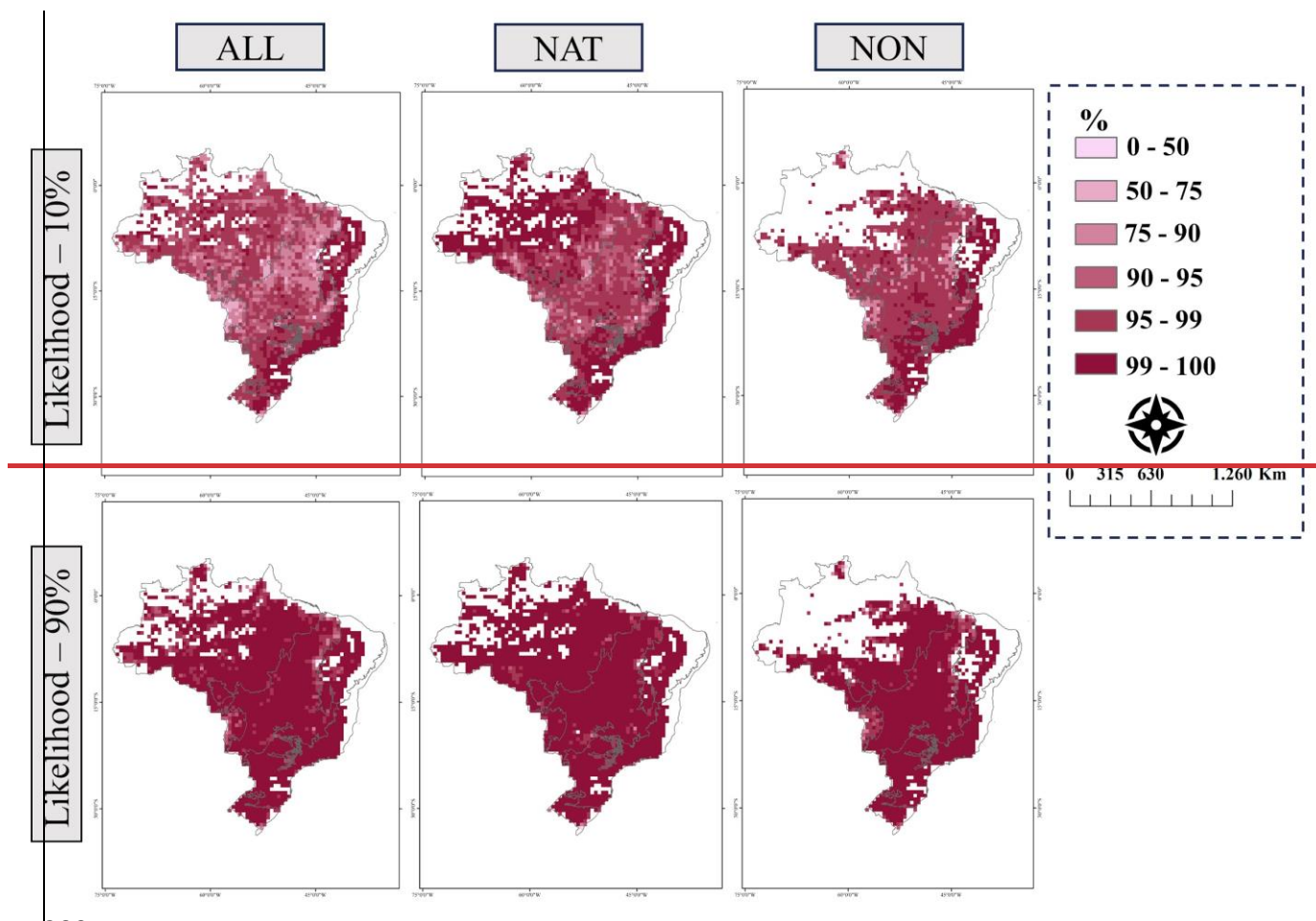
568

570

577

578

579 Despite the high likelihood associated with the observations, the model simulations exhibit a

580 certain degree of bias across the three categories (Fig. 7). A mean bias near 0.5 indicates no

581 bias, as the observations fall in the middle of the model's distribution. Amazonia and Cerrado

582 showed mean biases of 0.28 and 0.29 for ALL respectively, indicating an overestimation by

583 the simulations at lower burned areas. The Atlantic Forest presented a mean bias of 0.51,

584 suggesting that, overall, the model is unbiased although some pixels may still be biased.

585 Similarly, Pampa (0.42) and Caatinga (0.61) showed values near 0.5, indicating a lower degree

586 of bias. In contrast, a mean bias of 0.17 in the Pantanal suggests an overestimation of burned

587 area by the model, especially at lower levels. However, the model can distinguish between

588 lower and high burned areas in Pantanal (Fig. 5), indicating its ability to identify periods and

589 locations of more extreme burning, even if it does not exactly capture the correct magnitude.

590

591 Generally, higher uncertainties are observed for NAT and NON simulations, but a notable

592 improvement in bias is evident when compared to the ALL simulations. In the NAT

593 simulations, the model achieved its most favorable outcomes in Pampa (0.53) and Amazonia

594 (0.40), with the Pantanal also showing a noticeable improvement (0.34). The biases of 0.74 in

595 Caatinga and 0.72 in the Atlantic Forest indicate a trend toward underestimation in this fire

596 category. In Cerrado, a bias value of 0.33 was observed for NAT, aligning with the pattern seen

597 in the ALL simulations and suggesting a consistent overestimation, particularly for lower

598 burned areas.

599

600 In the NON simulations, Amazonia exhibited a bias of 0.38 but overestimated lower burned

601 areas. Cerrado and Pantanal showed similar patterns to those in the NAT simulations, with

602 respective mean biases of 0.36 and 0.31. The model tended to underestimate burned areas in

603 the Caatinga (0.81), particularly at higher burned areas. While Atlantic Forest (0.58) and Pampa

604 (0.59) showcased the most unbiased simulations for the NAT fire category, slight

605 underestimation of burned areas were noted in some instances (Fig. 87).
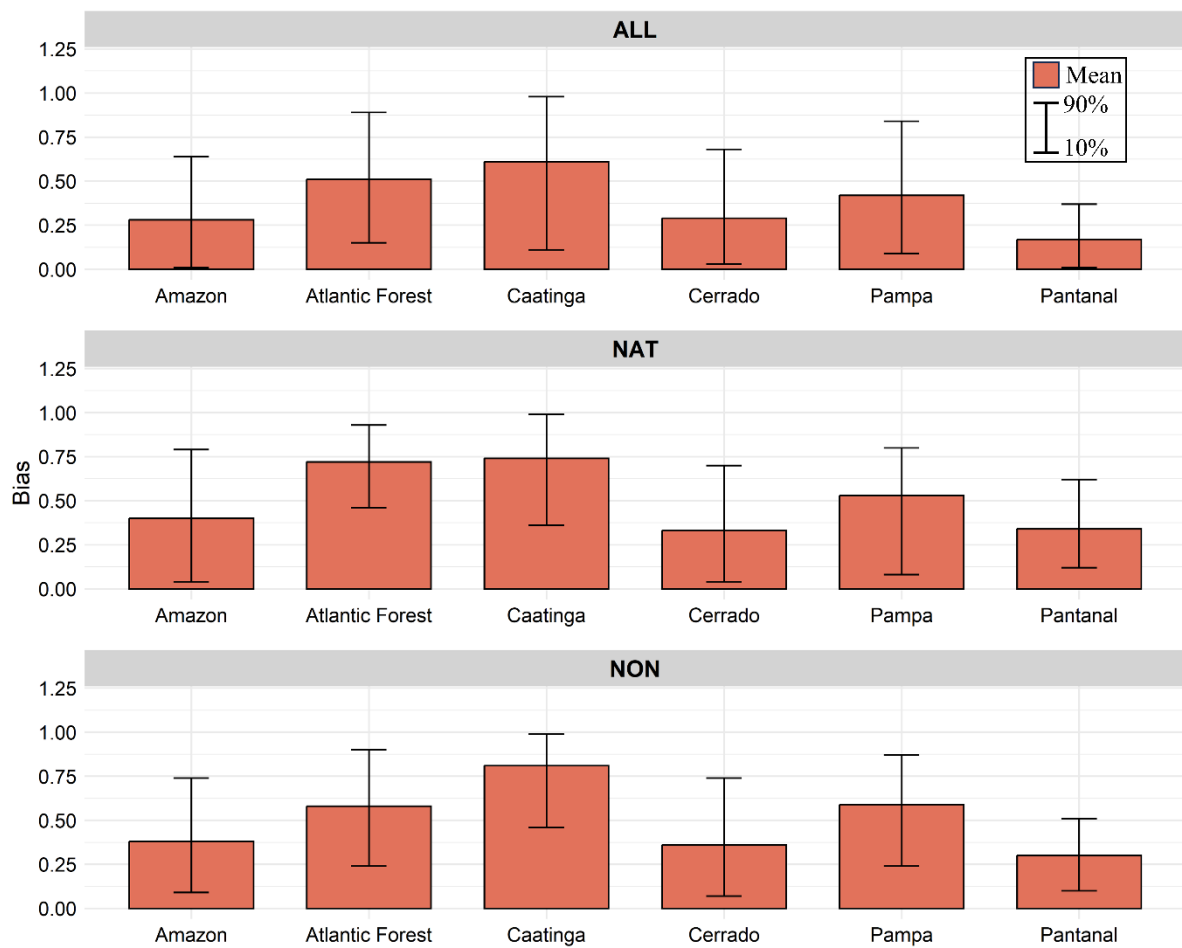
606

The spatial distribution of the mean bias, as depicted in Fig. 87, exhibits considerable variation. Pixels without values indicate zero burned area in the observations, where, by definition, the observation will always fall at the 0th percentile of the model posterior distribution. Consequently, the bias metric does not provide meaningful information for these pixels. The p-values reveal that in numerous areas, the bias is not statistically different from 0.5 (p-value > 0.05; indicated by brown color), suggesting unbiased simulations in these regions. SpecificallyFor example, lower fires in Amazonia tend to occur in areas of natural vegetation, where NAT simulations exhibit a non-significant bias. In these regions, ALL simulations tend to overestimate burned area. In southeastern Amazonia, fires were underestimated across all three fire categories, especially for NAT.

In Caatinga, all three simulations exhibited similar performance, significantly underestimating fires, particularly in the northern part of the Biome. The Atlantic Forest displayed better results

625   for both ALL and NON, with a substantial area exhibiting non-significant bias. The fragmented

626   landscape of this Biome likely limits data availability for NAT, possibly explaining the lower

627   performance in this fire category. In contrast, Cerrado demonstrated a consistent pattern across

628   all three fire categories, predominantly overestimating fires, especially in the south and

629   northeast. While some underestimation occurred in the central biome, it was mostly non-

630   significant. In Pantanal, the simulation consistently overestimated burned area across all three

631   categories, with ALL simulations showing significant overestimation throughout the Biome.

632   Finally, Pampa displayed a non-significant bias across̶ most of the region, except for the

633   northwest, where the model underestimated burning in all three simulations.

634

635

636
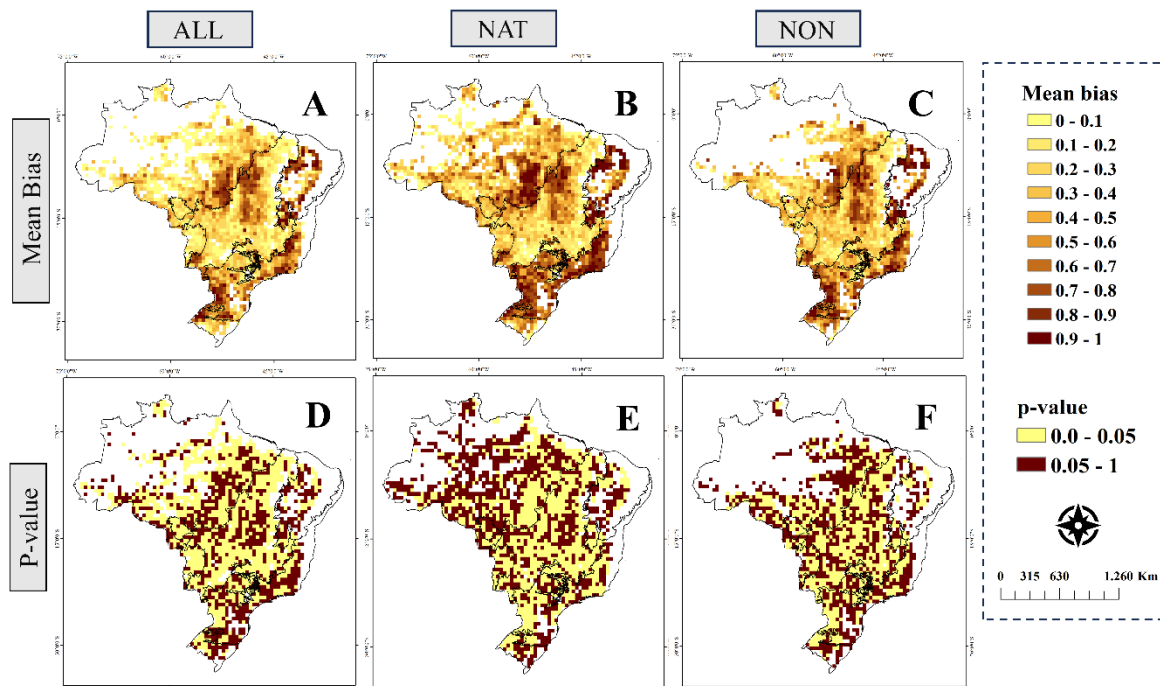
**Figure 87: Top row: Spatial mean bias of the modeled burned area to total area (ALL, (left),
natural vegetation area (NAT, (middle) and non-vegetation area (NON, (right). Bottom row:
Significance of the mean bias considering a 95% confidence level (p-value < 0 .05). Pixels
with p-value > 0.05 (brown color) are not significantly different from 0.5 mean bias meaning
that they are unbiased.**

3.2 Response of the modeled burned area to the explanatory variables

645   We assessed the potential and Sensitivity responses of the explanatory variables (Fig. 9-12 8,

646   9 and 10). The potential response offers insights into changes in burned area when the

647   explanatory variables deviate from the median, thereby identifying areas where responses tend

648   to drive or suppress burning. In contrast, the sensitivity response provides information on how

649 marginal changes in explanatory variables affect burned area (Kelley et al. 2019). Together,

650 these analyses highlight areas susceptible to more extreme burning (i.e., where the burned area

651 is sensitive to explanatory variables that tend to cause higher potential burning).

652

653 For ALL ~~burned area (Fig. 8)~~, ~~variations of~~ Group 1 (Maximum Temperature and Precipitation)

654 ~~from the median~~ is very likely to lead to an increase in the burned area in 62.33% (Fig. 9) of

655 Amazonia (~~with a~~ likelihood > ~~of over~~ 80%). This means that when these explanatory variables

656 assume their actual values in this Biome, the burned area tends to be higher, especially in the

657 ~~with increases up to 1% in the western edge and 10% in the north,~~ northeastern and southern

658 portions (Fig. 10) ~~southeastern of the biome~~. Conversely, these variations contributed to a

659 reduced burned area in 33.57% of Amazonia, predominantly observed in the western and

660 central areas, suggesting that Maximum Temperature and Precipitation tend to suppress burned

661 area in these regions. In 4.08% of the biome, the influence of Group 1 explanatory variables

662 on burned areas is not confidently predictable in terms of whether they will lead to an increase

663 or decrease (~~with~~ likelihood between 40% and 60%). ~~, and the model showed strong confidence~~

664 ~~only in the regions where these explanatory variables are major drivers and suppressors of~~

665 ~~burning~~. Our results indicate that the entire Amazonia is highly sensitive to minor variations in

666 Group 1 variables for ALL (Fig. 10~~8~~). Nonetheless, the middle and western regions tended to

667 be up to three times less sensitive than the rest of the biome.

668

669 In the Atlantic Forest, approximately 63.33% of the biome will likely experience an increase

670 in burned areas due to group 1 ~~when Temperature and Precipitation assume their real vs median~~

671 ~~values~~, mostly limited to 1% extra burning. This small increase highlights that these drivers do

672 not have a major influence on driving high levels of total burned area. Reduction of burned

673 area is observed in the western portion, encompassing 31.79% of the biome. ~~Uncertainties~~

674 ~~linked to Group 1 explanatory variables were found in 4.87% of the Atlantic Forest. Moreover,~~

675 ~~t~~This biome showed an overall lower sensitivity to climate.

676

677 In Cerrado, Group 1 is likely to drive burned area ~~up to 6%~~ in 58.30% of the biome, primarily

678 in the eastern part. Conversely, 37.16% of Cerrado is expected to ~~observe~~ experience a reduced

679 burned area. ~~by up to 10%, highlighting showing quite a~~the range in the ~~of~~ influence of this ~~in~~

680 ~~mean burned area from the~~explanatory variable group ~~on mean burned area~~. For ~~T~~the remaining

681 4.53% of the area, the influence of Group 1 is less clear, as no consistent pattern of increase or

682 decrease in burned area could be detected ~~remains uncertain~~. Cerrado exhibited high sensitivity

to changes in Group 1, except for the central region of the biome, which showed comparatively lower sensitivity. In the Pantanal, the central and northern areas are likely to experience an increase in burned area ~~by up to 1%~~ due to variations in Group 1, accounting for 51.92% of their total area. Conversely, the borders of the Pantanal, particularly the south, exhibited a reduction in burned area (42.30% of the Pantanal). ~~Approximately 5.76% of the Pantanal landscape remains uncertain regarding the direction of changes~~. The entire biome presented considerable sensitivity for small variations in Group 1. Pampa exhibited a high likelihood of increased burned area in 70.14% of the region with the west and ~~, mainly limited to 1%. We found a high likelihood of reduction in 26.86% of Pampa, located in the northwestern, and in 2.98% of the biome it is unclear the direction of changes. Pampa's west and~~ southeastern edges ~~showed to be~~ more sensitive to Group 1. The southern and eastern portions of Caatinga are likely to face an increase in burned area in ~~by up to 4%, affecting~~ 51.23% of the biome and a reduction in 47.34%. ~~, attributable to the influence of Group 1. Conversely, 47.34% of Caatinga, particularly in the northern and western, is more likely that the burned area will diminish, while 1.41% is unclear.~~ In general, the biome showed less sensitivity to Group 1, with slightly higher sensitivities observed in the central and northeast of the biome.

~~For~~ Group 2 ~~explanatory variables~~ (Edge Density and Road Density)~~,~~ is likely to drive increased burned area in 47.37% of Amazonia, . ~~will likely experience an increase in burned area when these explanatory variables deviate from the median. This increase is predominantly limited to 1%, concentrated~~ mainly in the western, central, and northeast regions. Conversely, areas with higher edge and road densities show a reduced burned area ~~of up to 11%,~~ covering 51.82% of Amazonia. ~~This is a 12% range in burned area, substantial for a fire-sensitive biome.~~ Overall, the biome displays moderate sensitivity to minor variations in Group 2, with higher sensitivity observed along its borders. The response in the Atlantic Forest exhibited more uncertainty in the 10th and 90th percentiles. Still, the likelihood indicates that 42.30% of the biome will likely experience increased burned areas of up to 2%, primarily located in the north and eastern edges. ~~Small reductions are found in 54.87% of the biome, limited to 0.2%.~~ Regions where increases are more likely also demonstrate greater sensitivity to Group 2, showing the potential for these drivers to have a disproportionate influence on extreme levels of burning.

~~The~~ Cerrado ~~biome~~ exhibited high spatial variability in response to Group 2, with a nearly equal mix of pixels where an increase (47.28%) and decrease (44.56%) in burned area is more likely to occur~~, both limited to 2.5%.~~ The northeast of the biome displayed higher sensitivity

to Group 2. In Pantanal, the central and southern regions are more likely to experience a decreased burned area, encompassing 53.84% of the biome. However, an increase is found in 42.30% of Pantanal~~, limited to 8%~~. The Pantanal demonstrated sensitivity to Group 2, especially in the north. In Pampa, 47.76% of the region exhibited increased burned areas, while reductions occur in 47% of it. ~~Increases reached up to 4%, primarily in the western portion.~~ These regions where an increase is likely also showed higher sensitivities. In Caatinga, a reduction in burned area is likely to occur in 50.17% of the biome, while an increase is expected in 38.86% of it. ~~Approximately 10.95% of the biome remains uncertain about the direction of change. In areas where results do suggest a confidence change, increases are mainly located in the middle of the biome.~~

In the context of Group 3 explanatory variables (Forest, Pasture, and Carbon in dead vegetation), approximately 53% of Amazonia will likely experience larger burned areas, primarily concentrated in the arc of deforestation (along the southern and eastern edges of the Amazonia). ~~, reaching up to 10%. Conversely, reductions are observed in 42% of the biome, with 4.23% remaining uncertain.~~ While displaying less sensitivity to minor changes than other groups, certain areas such as the cross borders with Cerrado and north exhibit higher sensitivity within the biome. In the Atlantic Forest, increased burned areas are observed in 41.53% of the region. ~~, while reductions are noted in 54.87%.~~ Decreases ~~in the biome~~ are primarily observed in the central southern and eastern areas. ~~, with magnitudes reaching up to 0.7%.~~ Overall, the sensitivity in this biome is lower although the spatial variation shows heightened sensitivity in the 90th percentile for some pixels across the biome.

In ~~the~~ Cerrado ~~biome, burning in the middle south and northeast edges is not likely driven by Group 3 variables, covering 54.83% of the biome. Conversely,~~ the north, northeast, and part of the south (39.72% of Cerrado) may experience increased burned areas ~~of up to 10%.~~ Regions with higher likelihood of increase also demonstrate greater sensitivity to ~~small variations in~~ Group 3. Pantanal shows approximately 30.77% of its area likely to experience ~~up to a 10%~~ increase in burned areas, mainly in the north and southeastern regions. ~~Conversely, edges and the southern part are more prone to reductions, encompassing 55.76% of the biome, while 13% remain uncertain. Pantanal~~ The biome demonstrates high sensitivity overall to Group 3. In Pampas, 52.23% of the region is more likely to see increased burned areas with ~~of up to 3.5%, while reductions are observed in 44.77% of the area.~~ ~~t~~The western part and eastern edges ~~of the biome~~ showing greater sensitivity to ~~minor changes in~~ Group 3. In Caatinga, approximately

~~53.35% of the biome is likely to experience reduced burned area while~~ 38.16% of the biome is likely to ~~increase burned area~~ ~~see up to 3% increases~~. The central and northeast regions, where increases are expected, also exhibit higher sensitivity to minor shifts in Group 3.
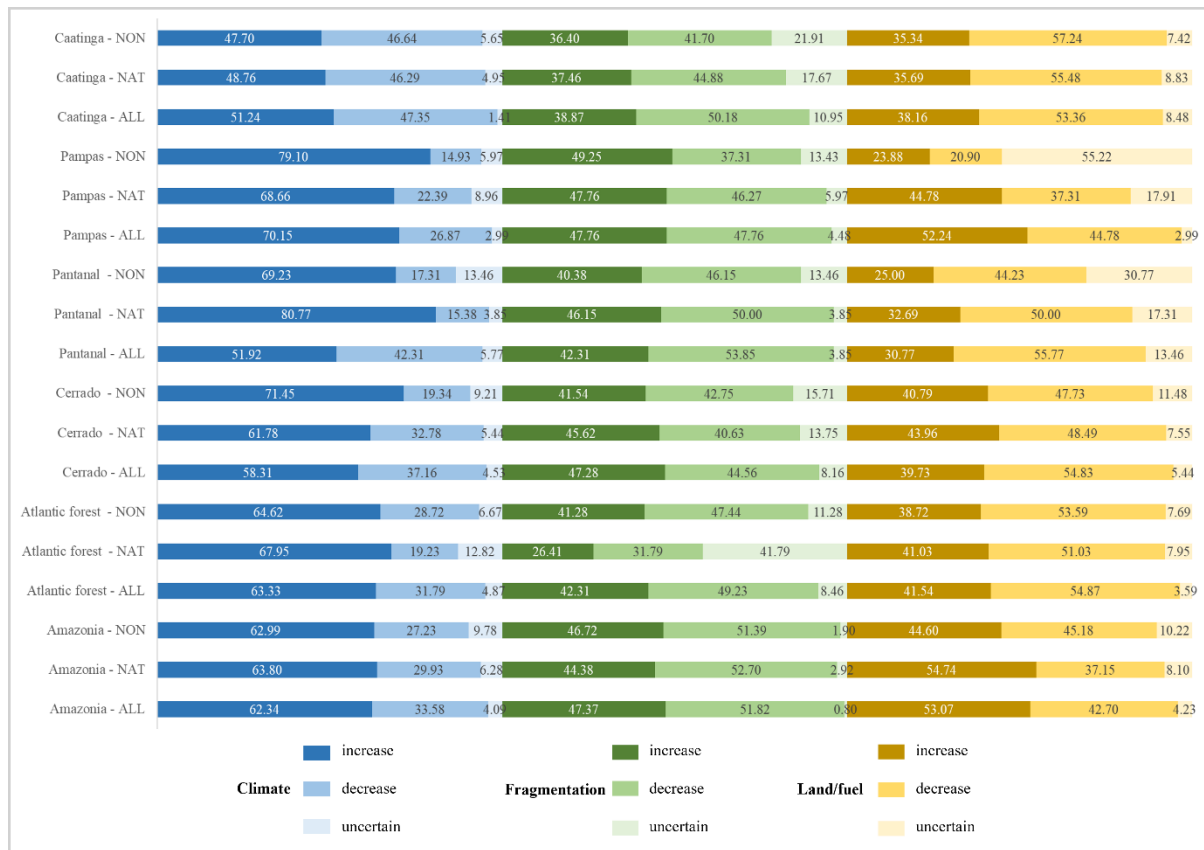
Figure 9: Percentage of burned area increase, decrease and uncertainty driven by climate (Group 1: Maximum Temperature and Precipitation), Fragmentation (Group 2: Road and Edge densities) and Land/fuel (Group 3: Forest, Pasture and Carbon in dead vegetation) for each biome (Amazonia, Atlantic Forest, Cerrado, Pantanal, Pampa and Caatinga) and fire category (ALL, NAT and NON).

762
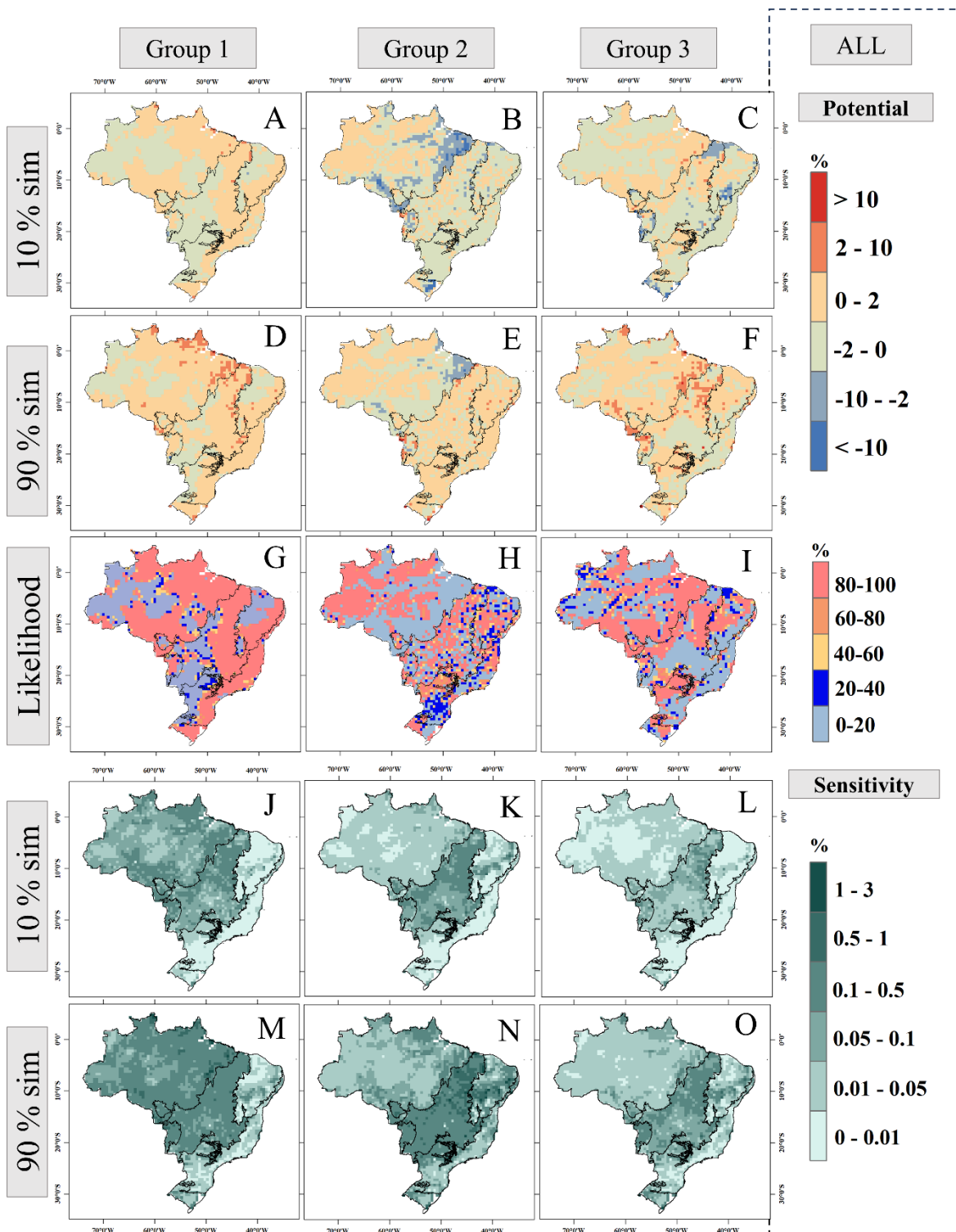
Figure 108: Response maps to ALL displaying the potential 10h percentile (first row), 90th percentile (second row), likelihood (third row) and sensitivity responses 10th percentile (fourth row) and 90th percentile (fifth rows). Each column presents the results for ~~one g~~**Group 1 (Maximum Temperature and Precipitation), Group 2 (Edge density and Road density), and Group 3 (Forest, Pasture, and Carbon in dead vegetation) of explanatory variables.**

Similar spatial patterns to ALL were observed for NAT when considering Group 1 across all biomes (Fig. 119). In the Amazonia, Group 1 will likely increase burned area in 63.79% of the biome. Areas with ~~Reductions are found in 29.92%, while 6.27% display an unclear response.~~ ~~This indicates a 2% increase in areas with~~ uncertain responses increased by 2%, particularly in the southeastern region of the Amazonia. Sensitivity analysis reveals that the borders of the Amazonia are more sensitive to Group 1, whereas areas with forest cover < 83% (Fig. 3) exhibit lower sensitivity. In the Atlantic Forest, Group 1 is likely to drive burned area increased in ~~changes~~ in 67.95% of the biome. Conversely, ~~19.23% is likely unaffected by Group 1, with~~ 12.82% remain~~ing~~ed unclear, representing an 8% increase compared to ALL. The Sensitivity to Group 1 was similar to ALL, generally lower for this biome.

In Cerrado, Group 1 ~~contributes to~~ increased burned area in 61.78% of the biome. ~~However, in 32.78% of the area, Group 1 is likely not a driving factor for the burned area, and in 4.53%, the response is unclear.~~ The biome also exhibits sensitivity to minor variations in Group 1 for NAT, albeit slightly lower in some areas ~~(Fig. 9)~~ than ALL. In Pantanal, 80.76% of its area likely has Group 1 as drivers of burned area in NAT, representing an increase of almost 30% compared to ALL. ~~Areas not influenced by this group decreased by 25% compared to ALL (15.38% of Pantanal), while 3.84% remains unclear.~~ The sensitivity analysis closely resembled ALL, with the entire biome significantly responding to variations in Group 1. In Pampas, it is likely that variations from the median lead to increased burning in 70.14% of the biome. Sensitivity is similar to ALL, primarily in the west but generally lower. Caatinga follows a similar pattern to ALL, with Group 1 influencing burning in 48.76% of the biome. Uncertainty increased to 4.94% of the biome, and sensitivity is similar, affecting mainly the middle and northeast regions.

For Group 2, Amazonia presented a more uncertain response between the 10th and 90th percentiles. However, the likelihood showed a marked pattern very similar to ALL where 47.37% of the biome has Group 2 as a driver of burning. Similar to Group 1, the sensitivity was lower in highly forested areas. For NAT, the Atlantic Forest showed large areas with an unclear response ~~(Fig. 9)~~, covering 41.79% of the biome. The areas where burning is likely to be driven by Group 2 encompasses 26.41%, a reduction of 15% when compared to ALL. The sensitivity was similar to ALL, with slightly higher values in some pixels. The Cerrado showed variation within the biome, with 45.61% of its area identified as potentially driven by Group 2 in NAT. While the sensitivity was lower than in ALL, it remained significant within Cerrado.

Pantanal exhibited Group 2 as a driver of burning in 46.15% of the biome, displaying a spatial pattern for the likelihood very similar to ALL. However, sensitivity was lower in the middle of Pantanal compared to the North and edges. Similarly, Pampa presented a response similar for ~~both~~ potential and sensitivity as in ALL, with 47.76% of areas likely to experience increased burning driven by Group 2. In Caatinga, areas likely to experience increased burning accounted for 37.45% of the biome, and the regions with unclear responses were 6.72% higher than in ALL (17.67%). Sensitivity showed the same pattern as in ALL.

In Amazonia, the areas with unclear responses to Group 3 ~~showed a~~increased from 4% ~~increase in areas with unclear responses for Group 3~~ to 8.10% ~~compared~~ in the~~to~~ ALL category. Meanwhile, ~~R~~regions where Group 3 is likely to drive an increase in burned area accounted for ~~susceptible to burning due to this group totaled~~ 54.74% of the biome. Densely forested areas also exhibited lower sensitivity to minor shifts in Group 3. In Atlantic Forest, Group 3 is likely to be a driver of burned area in 41.02% of the biome, very similar to ALL (41.53%). ~~Similarly,~~ ~~T~~the sensitivity followed the spatial pattern of ALL with an overall lower sensitivity. ~~presenting slightly higher in some pixels.~~ Areas prone to burning in ~~the~~ Cerrado due to Group 3 reduced by 10.84% compared to ALL, totaling 43.95% ~~compared to ALL~~. The reduction was concentrated in the northeast, while in the southwest there was an increase in the likelihood of burning due to Group 3. The sensitivity reduced in the northeast, varying across the biome. Within the Pantanal, regions susceptible to burning due to Group 3 comprised 32.69% of the area. Regions with an unclear response increased by 4.30%, encompassing 17.30% of the region and concentrated in the eastern edges.

In Pampas, 44.77% of the biome is likely to burn due to Group 3. ~~, while 17.30% of the biomes showed an unclear response~~. The sensitivity pattern for NAT followed ALL, concentrated in the western and eastern edges. The Caatinga accounted for 35.68% of areas prone to burning, with higher sensitivities observed in the middle and eastern regions of the biome.
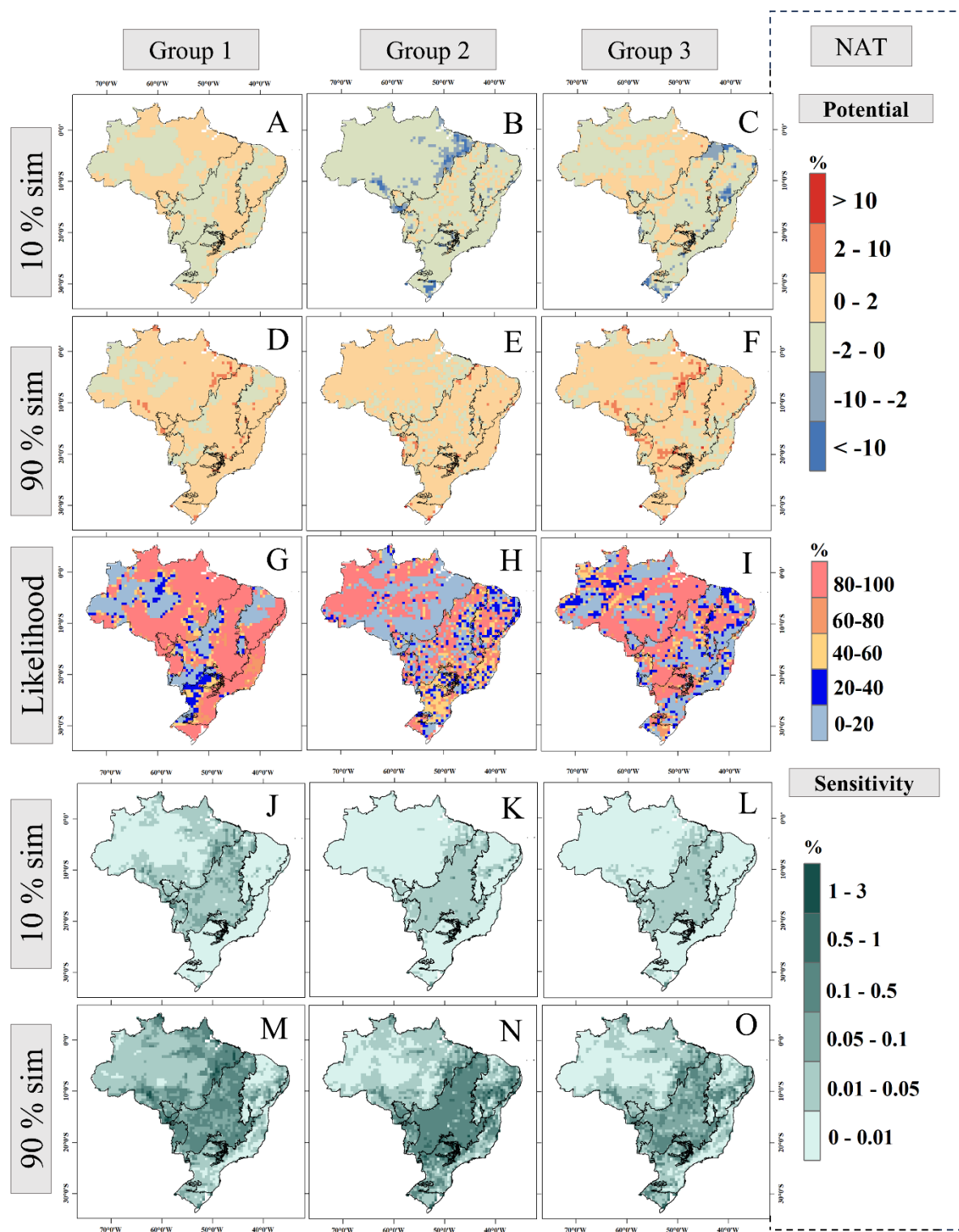
Figure 119: Same as Fig. 1089 but for NAT.

Higher uncertainties were found in the potential response for NON, meaning that the range of possible outcomes was generally larger for this category (Fig. 120). However, the likelihood showed similar spatial variation, although unclear responses increased. Group 1 acts as a driver of burning in 62.99% of Amazonia, a similar number when compared to NAT and ALL. The

845   main difference for this category is the magnitude of increase, which is higher at the edges and

846   in the middle of the biome. Likewise, the sensitivity was higher, especially in the 90th

847   percentile. The potential and sensitivity response of the Atlantic Forest was quite similar for

848   the three categories, with 64.61% likely to have Group 1 increasing burning in the biome.

849   Within the Cerrado, a 13.15% and 9.67% increase in areas susceptible to burning is observed

850   compared to ALL and NAT respectively (totaling 71.45%). Unclear responses were higher and

851   reached 9.21% of the biome. Sensitivity was higher in the northeast of the biome. For Pantanal,

852   NON comprised 69.23% of areas likely to burn due to Group 1. An increase in unclear

853   responses of 7.7% and 9.62% compared to ALL and NAT respectively was found (totaling

854   13.45% of the biome). ~~The magnitude of increase was also higher for NON~~. Sensitivity levels

855   were mostly high across the biome. Within Pampas, 79.10% of the biome was considered likely

856   to burn due to Group 1. The sensitivity was larger at the edges of the biome. The potential and

857   sensitivity responses of Caatinga followed a similar pattern between the categories, where

858   47.70% of the biome is likely to be susceptible to burning due to Group 1.

859

860   Similarly, the main difference for Group 2 in Amazonia was the increase, which reached up to

861   10% in the North and middle of the biome. Most of the biome shows high sensitivity. Within

862   the Atlantic Forest, there was a notable reduction of 30.51% in regions with unclear responses

863   compared to the NAT, where the proportion was 11.28%. Regions likely to increase burned

864   area due to fragmentation comprise 41.28% of the biome, an increase of 14.87% compared to

865   NAT. Sensitivity showed a similar pattern for the three categories where regions likely to

866   increase burning presented higher sensitivities. In Cerrado, approximately 41.54% of its area

867   is likely susceptible to increased burning due to group 2~~fragmentation, with 15.70% exhibiting~~

868   ~~unclear responses.~~ Higher sensitivity was observed in the northeastern region of the biome.

869   Pantanal showed a 40.38% likely increase and a significant sensitivity across the biome.

870   Pampas patterns for potential and sensitivity responses were similar to ALL and NAT, with

871   49.25% of the biome likely to increase burning. However, the likelihood was comparatively

872   lower (between 60% and 80%). For Caatinga, it is likely to increase burning in 36.39% of the

873   biome.~~, while the regions with unclear response reached 21.90%.~~ Sensitivity displayed a

874   similar pattern to ALL and NAT with higher sensitivities in the middle and northeast.

875

876   Group 3 exhibited higher uncertainties in Amazonia ~~between the 10th and 90th percentiles~~.

877   The likelihood of increase encompasses 44.59% of the biome, while areas with unclear

878   responses surpass ALL and NAT, comprising 10.21%. Sensitivity was also higher, especially

879   in the north of Amazonia. The Atlantic Forest showed a similar pattern compared to ALL and

880   NAT with 38.71% of its area likely to increase and generally lower sensitivity to this group.

881   Cerrado exhibited a marked pattern, where burning in the north is likely driven by Group 3,

882   encompassing 40.78% of the biome. These regions also exhibited higher sensitivity to ~~minor~~

883   ~~variations in~~ Group 3. ~~Unclear responses were identified in 11.48% of the biome.~~ This Group

884   exhibited the highest level of unclear response in the Pantanal, totaling 30.77%. Meanwhile,

885   regions with a likelihood of increased burning decreased to 25%. The sensitivity was generally

886   high across the biome. This group also showed to be highly uncertain in Pampas~~, with~~ (55.22%

887   of the biome) ~~of the biome presenting unclear responses~~. The areas likely to increase burning

888   comprised 23.88% of Pampa, a reduction of 28.35% and 20.89% compared to ALL and NAT,

889   respectively. The sensitivity was similar in the three categories with slightly higher sensitivity

890   in the middle for NON. The Caatinga region exhibited a 35.33% portion of its area with a

891   heightened likelihood of increased burning attributed to Group 3, displaying a similar pattern

892   across all three categories concerning potential and sensitivity response.

893
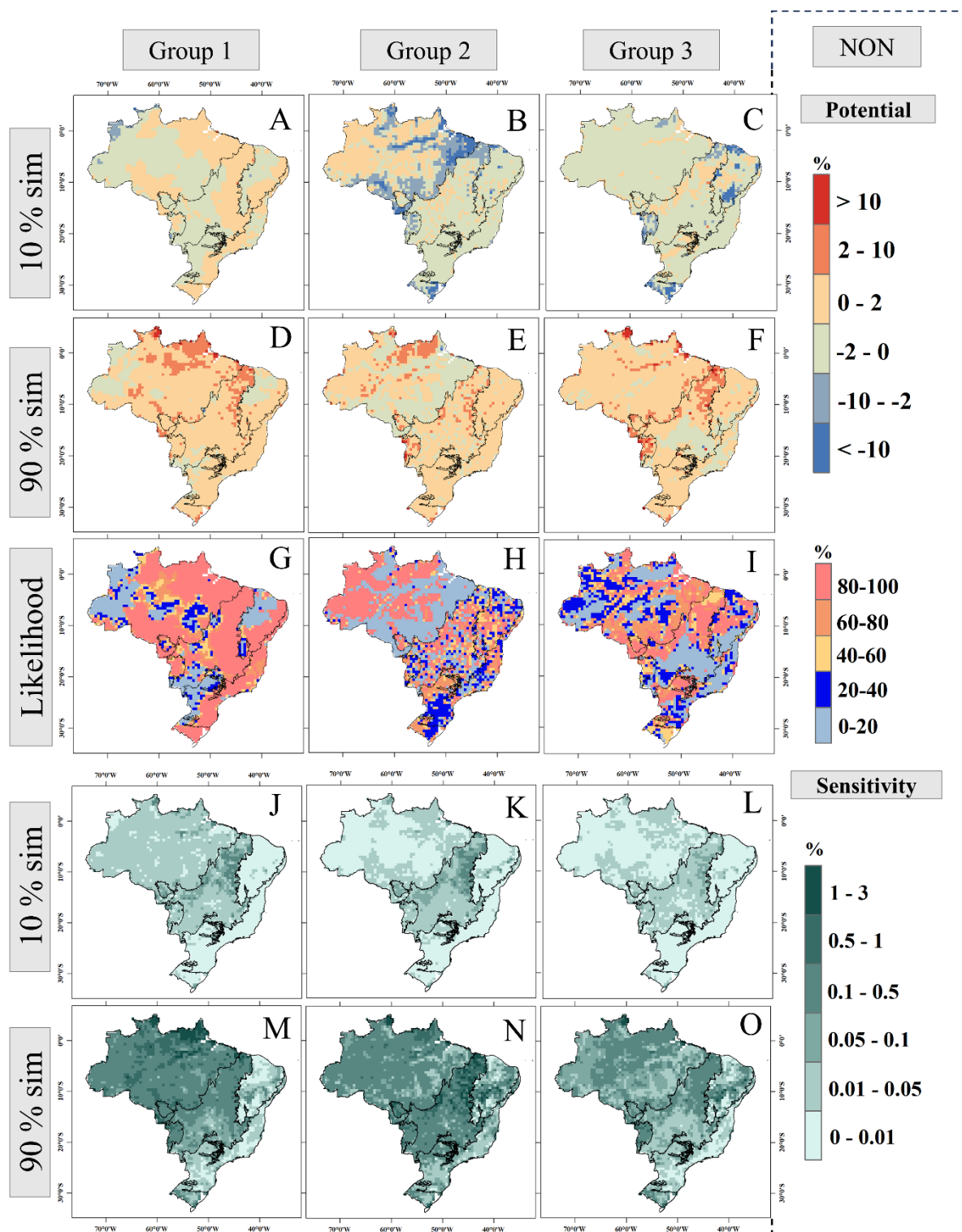
Figure 11~~0~~: Same as Fig. ~~108~~9 but for NON.

4 DISCUSSION

4.1 FLAME's performance in context

Our proposed model uniquely combines two previously distinct approaches employed in fire modeling: Bayesian inference and Maximum Entropy (Kelley et al., 2021; Ferreira et al., 2023). This combination allows for a more comprehensive understanding of fire dynamics as it models a probability distribution rather than singular values, a departure from conventional models (e.g. Bistinas et al., 2014; Haas et al., 2022 ~~Hantson et al., 2016; Rabin et al., 2017~~). Notably, our approach employs Maximum Entropy to capture the most uncertain outcomes that align with our priors, reflecting the stochastic nature of real-world fires. This concept contributes to a more nuanced and realistic representation of fire behaviour. We conducted our analysis by categorizing the burned area into three categories: ~~fires in~~ burned areas in both natural and non-natural vegetation (ALL), ~~fires reaching~~ burned areas in natural vegetation (NAT), and ~~fires reaching~~ burned areas in non-natural vegetation (NON). This classification yielded distinct results for each category with an overall improvement across the biomes for the NAT and NON. Moreover, this approach allows us to make more targeted conclusions.

The results demonstrate the robust performance of our model in capturing observations while providing a range of possible outcomes represented by the 10th and 90th percentiles. It is noteworthy that the model was capable of reproducing the observations in Pampa, Atlantic Forest and Caatinga, as these are areas where other methods used in previous studies have not performed well (Nogueira et al. 2017, Oliveira et al., 2022). Despite some level of bias in the results, even during periods of suboptimal performance, the likelihood of the observations remained consistently high, with the majority exceeding 80%. The Pantanal biome presented an exception, displaying a likelihood of 59% for the combined category (ALL), with improvement for specific categories, reaching 86% for NAT and 78% for NON. This biome encompasses a mosaic of vegetation types characterized by seasonally flooded areas which plays an important role on the fire dynamics of the region (Damasceno-Junior et al.,2021). Fire in these areas were not included in this study due to our general approach, posing a limitation for simulation within this biome. However, our framework's adaptability means that future work could look at different explanatory variables, relationship ~~variables~~ and fire categorizations that could target performance in places like the Pantanal.

The MaxEnt species distribution model, which uses the same Mmaximum Eentropy concept applied here, became quite popular in fire modeling studies (e.g., Fonseca et al., 2017; Banerjee, 2021; Ferreira et al., 2023). However, the MaxEnt software provides default settings, based on average values which are likely to change according to species, study region and environmental data (Phillips and Dudik, 2008). Additionally, these current settings are estimated to result in excessively complex models, potentially leading to overfitting (Radosavljevic and Anderson, 2013). When employing MaxEnt, it is crucial to utilize independent evaluation data (Peterson et al., 2011) such as that used in the present study. However, many studies assess performance by randomly partitioning occurrence data into calibration and evaluation datasets (Chen et al., 2015; Göltas et al., 2024). This procedure limits the ability to obtain reliable estimates of model performance, generality, and transferability. Finally, the area under the receiver operating characteristic (ROC) curve, commonly known as AUC, is widely used as a standard method to evaluate the accuracy of maximum entropyMaxEnt-based models. Nonetheless, this measure does not provide information about the spatial distribution of the model's performance (Lobo et al., 2007; Jiménez-Valverde, 2011) which also potentially masks the spatial variability of the explanatory variables contribution to the model.

The MaxEnt species distribution model, widely used in fire modeling (e.g., Fonseca et al., 2017; Banerjee, 2021; Ferreira et al., 2023), applies the same maximum entropy concept as in this study. However, MaxEnt's default settings, based on average values, may not suit specific species, regions, or datasets (Phillips and Dudik, 2008) and can result in overly complex models prone to overfitting (Radosavljevic and Anderson, 2013). While independent evaluation data is essential (Peterson et al., 2011), many studies rely on random partitions of occurrence data for calibration and validation (Chen et al., 2015; Göltas et al., 2024), which can compromise model reliability and generality. In contrast, our approach incorporates an independent evaluation framework designed to assess the model's capacity to capture unseen dynamics and simulate scenarios beyond the observed data. Furthermore, the commonly used AUC metric, while widely adopted, fails to provide insights into the spatial distribution of model performance (Lobo et al., 2007; Jiménez-Valverde, 2011). Here, we developed targeted evaluation analysis to assess model performance spatially

Currently, global fire models incompletely reproduce the observed spatial patterns of burned area. We found that FLAME captures high burned areaing events, albeit not with the exact magnitude observed. This ability presents an advantage compared to many process-based

969 ~~global~~ fire models. While global fire modeling provides useful information into broad-scale
970 patterns and trends, they are mostly designed to estimate global mean burned area (Hantson et
971 al., 2016; Burton and Lampe et al., 2023). As a result, its applicability to regional scales such
972 as the Brazilian biomes is inherently limited. These models often rely on assumptions about
973 the relationships between explanatory variables, ~~Furthermore, these models are typically~~
974 ~~constructed based on assumptions regarding explanatory variable relationships~~, which may not
975 hold true in all locations due to variations in environmental conditions, ecosystem dynamics,
976 and human activities. Additionally, while fire-enabled Earth System Models can integrate
977 feedback mechanisms between land and atmosphere, therefore enabling the evaluation of inter-
978 variable effects, offline global fire models do not. Similarly, ~~However, Earth System Models~~
979 ~~integrate feedback mechanisms between burned areas and~~ explanatory ~~predictor variables,~~
980 ~~enabling the evaluation of inter-variable effects.~~ FLAME is not designed to capture these
981 feedbacks, underscoring the need for tailored methodologies to address specific research
982 questions.

983

984 **4.2 Burning controls across the biomes**

985

986 We combined our explanatory variables into three groups to assess their compound effect on
987 the burned area. This is a similar approach to Kelley et al. (2019) who also used a Bayesian
988 framework to assess drivers of global fire regimes. Nonetheless, Kelley et al. (2019)
989 considered only linear responses which is especially challenging when considering the varying
990 responses across the globe. Our results highlighted the spatial variability of each explanatory
991 variable group's influence on burning within and between each biome. The potential response
992 displayed similar spatial likelihood variation between the ALL, NAT and NON categories.
993 However, differences were still observed, especially for the fire-dependent biomes (Cerrado
994 and Pantanal). Overall, the uncertainties were larger for the NON category, particularly for
995 Pampas and Pantanal.

996

997 For example, Group 1 (Maximum Temperature and Precipitation ~~(Group 1)~~) are likely drivers
998 of burning in large portions of each biome during the fire peak, as demonstrated by the potential
999 and sensitivity results. Our results indicate that in highly forested areas in Amazonia, climate
1000 alone does not control burning, suggesting that forests can potentially mitigate the effects of
1001 climate in burned area. These regions showed up to three times less sensitivity to minor
1002 variations of climate for NAT while ALL and NON displayed high sensitivity in the whole

biome. However, natural landscapes, especially forests, are highly susceptible during extreme weather conditions (Dos Reis et al., 2021; Barbosa et al., 2022). This suggests that while natural vegetation may mitigate sensitivity to minor climate variations, projected climate change could greatly increase the risk of the Amazonia forest fires (Flores et al., 2024). Moreover, non-natural vegetation in Amazonia is mainly concentrated in the arc of deforestation, reducing the samples for this category in other parts of the Amazonia and potentially influencing the model's response. In this sense, dividing the Amazonia into subregions, specifically separating the region where most deforestation occurs could improve the model's regional estimates and is a recommended approach for future Amazonia-focused research.

An opposite dynamic was found in Cerrado and Pantanal. Regions with large areas of natural vegetation were more likely to be influenced by climate. These regions were more sensitive to minor variations in climate for NON in Cerrado while the entire Pantanal displayed similar sensitivity in the three categories. This aligns with prior research showing that fires in Cerrado are linked with meteorological conditions, particularly rainfall and temperature (Nogueira et al., 2017; Libonati et al., 2022; LI et al., 2022). Similarly, in Pantanal, the 2020 fire season revealed the connections between meteorological conditions and increased burning in the biome (Barbosa et al., 2022; Libonati et al. 2022b) and again during the 2023 El Niño. Barbosa et al., (2022), reported that 84% of the 2020 record of fires in Pantanal occurred in natural vegetation, with a 514% increase from average within forests. Despite Althoughbeing a combination with land use changes played a role, the precipitation and maximum temperature anomalies were particularly high in 2020, contributing to the spread of fires into fire-sensitive vegetation.

Group 2 (Edge density and Road density) encompasses explanatory variables expected to have uncertain response across the biomes. Within Cerrado, 40.63% of its area will likely decrease burned area for NAT due to Group 2. A high density of forest edges has been associated with a higher incidence of fires in forest ecosystems (Armenteras et al., 2013; Silva-Junior et al., 2022). However, fragmentation can also act as a barrier to fire spread, potentially reducing fire occurrences (Driscoll et al., 2021). Rosan et al., (2022), revealed that in Cerrado, fragmentation correlates with a decrease in burned area fraction, while in Amazonia, it is linked to an increase in burning. Nevertheless, we found a decrease in burning where edge densities are concentrated in the Amazonia. This could indicate that the edges of the Amazonia are reaching a levels of fragmentation that may act as firebreaks, thereby are impedinged fires from spreading,

1037 ~~considering~~ particularly due to the reduction of aboveground biomass near forest edges
1038 (Numata et al., 2017). However, further research is needed to test this hypothesis.

1039

1040 Depending on the landscape, road densities can also exhibit contrasting relationships with fires.
1041 While more fires are expected surrounding roads (Armenteras et al., 2017), less fires are
1042 expected with increased density due to urbanization. The Atlantic Forest is a very fragmented
1043 biome with very high densities of natural edges and roads (Fig. 3). We found an uncertain
1044 response for NAT in 41.79% of the Atlantic Forest and only 26.41% likely to increase. Singh
1045 and Huang (2022) suggests that the fragmentation partly explains burned area variation in the
1046 Atlantic Forest where small patches are more vulnerable to fires. The majority of Caatinga is
1047 likely to decrease burning due to Group 2. However, the sensitivity was up to three times higher
1048 in the middle and northeast, which is more likely to increase. Antongiovanni et al. (2020)
1049 discussed that fires in Caatinga occur at all edge distances, although they are slightly more
1050 frequent at fragment edges. Nonetheless, the limited amount of studies across the different
1051 biomes addressing these relationships makes it harder to understand the related uncertainties.

1052

1053 Group 3 (Forest, Pasture, and Carbon in dead vegetation) is likely to influence burning in
1054 54.74% of Amazonia for NAT, particularly in the arc of deforestation. This suggests that the
1055 combination of less forest, increased pasture and more fuel (Fig. 3) increases burning in natural
1056 lands in Amazonia, corroborating previous findings (Silveira et al., 2020; Silveira et al., 2022).
1057 The relationship in Pantanal and Pampa showed that these variables increase burning in 32.69%
1058 (NAT) and 25% in Pantanal and 44.78% (NAT) and 23.88% (NON) for Pampas. The regions
1059 with unclear responses were the highest for NON, 30.77% of Pantanal and 55.22% of Pampa.
1060 These biomes are characterized by lower forest and pasture cover (Fig. 3) with fires and cattle
1061 ranching mainly linked to grasslands (Barbosa et al., 2022; Fidelis et al., 2022; Chiaravalloti et
1062 al., 2023). Thus, incorporating grassland cover in the model will likely reveal further
1063 relationships between burned area and LULC in these biomes. Caatinga showed increased
1064 sensitivity where Group 3 is likely to increase burning, matching the area of influence of Group
1065 2. This area is associated with low forest cover and ~~soil carbon~~carbon in dead vegetation and
1066 moderate pasture cover. Araújo et al. (2012), observed that due to the intermittent and scattered
1067 characteristics of cattle ranching in the Caatinga, fires tend to occur mainly in natural
1068 vegetation, characterized by large cover of savanna vegetation. Although our study provides a
1069 general overview of burning dynamics in the biomes, targeting variables is highly
1070 recommended in future studies, especially where fires are poorly understood as in Caatinga.

4.3 FLAME potentialities

Further developments are recommended to improve FLAME's capabilities. Exploring and incorporating better-informed and additional priors may constrain the explanatory variables' response uncertainties. Utilizing alternative metrics to assess drivers, particularly those tailored to specific biomes, could offer a more nuanced understanding of the influencing factors. It could also help improve biases in biomes such as the Pantanal. Customizing explanatory variable selection based on biome characteristics would also contribute to a more biome-focused and contextually relevant analysis. Consideration of different fire categories show how the model could be used in further research. For instance, a more detailed stratification could involve categorizing fires into distinct groups such as forest, agricultural, and deforestation fires. While deforestation data was not incorporated in this study, efforts should be made to integrate this valuable information where possible. Furthermore, accounting for the varying proportions of natural and non-natural lands within each pixel, as demonstrated in this study, provides a more accurate landscape representation. This contributes to improved simulations where these areas are very small. In addition, finer grids and the subdivision of the biomes may uncover local processes, though eventually fire spread between fine-scales would need to be considered. Understanding the factors that drive fires~~This~~ could be crucial for ~~understanding localized patterns and~~ improving the model's predictive capabilities. Previous~~erilous~~ modeling attempts often parameterize on a large regional basis. However, our approach allows for optimization on much smaller areas while still quantifying the confidence in the analysis. FLAME is flexible enough to be used in various locations and, through targeted benchmarking, holds the potential to evaluate extreme fires, inter-annual and seasonal variability of fires, project future fires, and simulate other hazards. With appropriate adaptations and enhancements, FLAME has the potential to evolve into a robust model capable of simulating terrestrial impacts effectively.

5 FINAL CONSIDERATIONS

The self-reinforcing cycle between fires and climate change makes it fundamental to improve fire simulations. An understanding of what drives fires is essential for devising mitigation and adaptation strategies. However, it can be particularly challenging due to the intricate interplay of various factors, especially in a diverse country like Brazil. We propose a novel approach for simulating burned area in the Brazilian biomes that keeps assumptions at a minimum whilst

quantifying uncertainties. The model performs well in all biomes, and enables the assessment of fire categories and the grouped effect of explanatory variables. Furthermore, conventional modeling efforts often parameterize at a large scale. FLAME enables optimization in smaller areas while still providing a means to quantify confidence in the analysis.

Climate is an important factor in burned area in all biomes. Despite several studies showing this relationship, climate-related uncertainties had not been extensively quantified, a gap this research fulfills. Groups 2 (road and edge densities) and 3 (forest, pasture and soil carboncarbon in dead vegetation) and the NON category showed the highest uncertainties among the responses. This highlights the challenge in modeling human-related factors. Pantanal, Cerrado, and Amazonia showed higher sensitivity to minor variations in the explanatory variables. It is important to note that sensitivity is more important where burning is already high, which is the case in these biomes (AlencarLENCAR et al., 2022). None of the groups drive huge changes in burned area in the Atlantic Forest. However, since this biome is fire-sensitive, even small changes in burned area can have a substantial impact on its ecosystems., though as it is fire-sensitive, it still can have a large impact. Uncertain responses compound the complexity of burned area drivers as different explanatory variables interact uniquely within each biome. The same vegetation type may show contrasting responses to the same drivers in different locations. Therefore, no universal fire management policies will fit the whole country. In particular, Caatinga, Atlantic Forest and Pampa require further investigation. Emphasizing regional-scale analysis is crucial for decision-makers and fire management strategies, enabling more informed and effective prevention of fires.

CODE AVAILABILITY

FLAME 1.0 model code is available at https://doi.org/10.5281/zenodo.13367375 (Barbosa et al., 2024a).

DATA AVAILABILITY

The data supporting this study is available at the Zenodo repository: https://doi.org/10.5281/zenodo.11491125 (Barbosa et al, 2024b).

AUTHOR CONTRIBUTIONS

Conceptualization: MLFB, DIK, CAB, LOA

Data Curation: MLFB, DIK, AB

Formal Analysis: MLFB, DIK

Methodology: MLFB, DIK, CAB

Resources/Software: MLFB, DIK, CAB

Visualization: MLFB

Funding acquisition: MLFB, LOA

Supervision: LOA, DIK, CAB

Resources: LOA, DIK, CAB

Writing – Original Draft Preparation: MLFB

Writing – Review & Editing: MLFB, IJMF, RMV, AB, PGM

All co-authors approved the draft

COMPETING INTERESTS

The authors declare that they have no conflict of interest.

FUNDING ACKNOWLEDGMENTS
DIK was supported by the Natural Environment Research Council as part of the LTSM2 TerraFIRMA project and NC-International programme [NE/X006247/1] delivering National Capability. This work and its contributors (CAB, AB) were funded by the Met Office Climate Science for Service Partnership (CSSP) Brazil project which is supported by the Department for Science, Innovation & Technology (DSIT). LOA acknowledges support by the São Paulo Research Foundation (FAPESP) (projects: 2021/07660-2 and 2020/16457-3) and by the National Council for Scientific and Technological Development (CNPq) project 409531/2021-9 and productivity scholarship (process: 314473/2020-3). MLFB and IJMF were supported by the Coordination for the Improvement of Higher Education Personnel (CAPES), Finance Code 001. MLFB and PGM acknowledges support by the São Paulo Research Foundation (FAPESP) (project: 2021/11940-0). RMV thanks the São Paulo Research Foundation (FAPESP) for grants 2020/06470-2 and 2022/13322-5.

ACKNOWLEDGMENTS
Eleanor Burke (UK Met Office) for original JULES-ES simulations.
Tristan Quaife (University of Reading) for supervisor support.
Eddy Roberton (UK Met Office) for support and discussion on this research.

REFERENCES

1187 ABRIL-PLA, O.; ANDREANI, V.; CARROLL, C.; DONG, L.; FONNESBECK, C. J.;
1188 KOCHUROV, M.; KUMAR, R.; LAO, J.; LUHMANN, C. C.; MARTIN, O. A.; OSTHEGE,
1189 M.; VIEIRA, R.; WIECKI, T.; ZINKOV, R. **PyMC: A Modern and Comprehensive**
1190 **Probabilistic Programming Framework in Python. Computer Science**, v.9, p. e1516, 2023.

1191 ALENCAR, A.A.; ARRUDA, V.L.; SILVA, W.V.D.; CONCIANI, D.E.; COSTA, D.P.;
1192 CRUSCO, N.; DUVERGER, S.G.; FERREIRA, N.C.; FRANCA-ROCHA, W.; HASENACK,
1193 H. AND MARTENEXEN, L.F.M. Long-term landsat-based monthly burned area dataset for
1194 the Brazilian biomes using deep learning. **Remote Sensing**, v.14, p.2510, 2022.

1195 ANDELA, N., MORTON, D.C., GIGLIO, L., CHEN, Y., VAN DER WERF, G.R.,
1196 KASIBHATLA, P.S., DEFRIES, R.S., COLLATZ, G.J., HANTSON, S., KLOSTER, S. AND
1197 BACHELET, D. A human-driven decline in global burned area. Science, v.356, p.1356-1362,
1198 2017.

1199 ANTONGIOVANNI, M.; VENTICINQUE, E.M.; MATSUMOTO, M.; FONSECA, C.R.
1200 Chronic anthropogenic disturbance on Caatinga dry forest fragments. **Journal of Applied**
1201 **Ecology**, v. 57, p.2064-2074, 2020.

1202 ARAGAO, L.E.O.; MALHI, Y.; BARBIER, N.; LIMA, A.; SHIMABUKURO, Y.;
1203 ANDERSON, L.; SAATCHI, S. Interactions between rainfall, deforestation and fires during
1204 recent years in the Brazilian Amazonia. **Philosophical Transactions of the Royal Society B:**
1205 **Biological Sciences**, v.363, n.1498, p.1779-1785, 2008.

1206 ARMENTERAS, D.; GONZÁLEZ, T.M; RETANA, J. Forest fragmentation and edge
1207 influence on fire occurrence and intensity under different management types in Amazon
1208 forests. **Biological Conservation**, v.159, p.73-79, 2013.

1209 ARMENTERAS, D.; BARRETO, J.S.; TABOR, K.; MOLOWNY-HORAS, R.; RETANA, J.
1210 Changing patterns of fire occurrence in proximity to forest edges, roads and rivers between
1211 NW Amazonian countries. **Biogeosciences**, v.14, p.2755-2765, 2017.

1212 BANERJEE, P., 2021. Maximum entropy-based forest fire likelihood mapping: analysing the
1213 trends, distribution, and drivers of forest fires in Sikkim Himalaya. Scandinavian Journal of
1214 Forest Research, 36(4), pp.275-288.

1215 BARBOSA, M.L.F., HADDAD, I., DA SILVA NASCIMENTO, A.L., MAXIMO DA SILVA,
1216 G., MOURA DA VEIGA, R., HOFFMANN, T.B., ROSANE DE SOUZA, A., DALAGNOL,
1217 R., SUSIN STREHER, A., SOUZA PEREIRA, F.R. AND OLIVEIRA E CRUZ DE
1218 ARAGÃO, L.E., 2022. Compound impact of land use and extreme climate on the 2020 fire
1219 record of the Brazilian Pantanal. Global Ecology and Biogeography, 31(10), pp.1960-1975.

1220 BARBOSA, M.L.F, KELLEY, D., BURTON, C. & ANDERSON, L. (2024a). malu-
1221 barbosa/FLAME: FLAME 1.0: Fogo local analisado pela Máxima Entropia (v0.1). Zenodo.
1222 https://doi.org/10.5281/zenodo.13367375.

BARBOSA, M.L.F, KELLEY, D., BRADLEY, A., & BURTON, C. (2024b). FLAME 1.0: a novel approach for modelling burned area in the Brazilian biomes using the Maximum Entropy concept - Input Data [Data set]. Zenodo. https://doi.org/10.5281/zenodo.11491125.

BISTINAS, I., HARRISON, S.P., PRENTICE, I.C., PEREIRA, J.M. Causal relationships versus emergent patterns in the global controls of fire frequency. Biogeosciences, 11(18):5087-101, 2014.

BURTON C, BETTS R, CARDOSO M, FELDPAUSCH TR, HARPER A, JONES CD, KELLEY DI, ROBERTSON E, WILTSHIRE A. Representation of fire, land-use change and vegetation dynamics in the Joint UK Land Environment Simulator vn4. 9 (JULES). Geoscientific Model Development. 2019 Jan 9;12(1):179-93.

BURTON C, KELLEY DI, JONES CD, BETTS RA, CARDOSO M, ANDERSON L. South American fires and their impacts on ecosystems increase with continued emissions. Climate Resilience and Sustainability. 2022 Feb;1(1):e8.

BURTON, C.; LAMPE, S.; KELLEY, D.; THIERY, W.; HANTSON, S.; CHRISTIDIS, N.; GUDMUNDSSON, L.; FORREST, M.; BURKE, E.; CHANG, J.; HUANG, H. Global burned area increasingly explained by climate change. **Preprint** at https://doi. org/10.21203/rs, 3. 2023.

CAMPANHARO, W.A., LOPES, A.P., ANDERSON, L.O., DA SILVA, T.F. AND ARAGÃO, L.E., 2019. Translating fire impacts in Southwestern Amazonia into economic costs. Remote Sensing, 11(7), p.764.

CANO-CRESPO, A.; OLIVEIRA, P. J.; BOIT, A.; CARDOSO, M.; THONICKE, K. Forest edge burning in the Brazilian Amazon promoted by escaping fires from managed pastures. **Journal of Geophysical Research: Biogeosciences**, v.120, p.2095-2107, 2015.

CECIL, D.J. **LIS/OTD 0.5 degree high resolution monthly climatology (HRMC).** Washington: NASA, 2006.

CHEN, F.; DU, Y.; NIU, S.; ZHAO, J. Modeling forest lightning fire occurrence in the Daxinganling Mountains of Northeastern China with MAXENT. **Forests**, v.6, p.1422-1438, 2015.

CHEN, X.; DIMITROV, N.B.; MEYERS, L.A. Uncertainty analysis of species distribution models. PloS One, v.14, e0214190, 2019.

CHIARAVALLOTI, R.M.; TOMAS, W.M.; AKRE, T.; MORATO, R.G.; CAMILO, A.R.; GIORDANO, A.J.; LEIMGRUBER, P. Achieving conservation through cattle ranching: the case of the Brazilian Pantanal. **Conservation Science and Practice**, 2023.

DOS REIS, M.; DE ALENCASTRO GRAÇA, P.M.L.; YANAI, A.M.; RAMOS, C.J.P.; FEARNSIDE, P.M. Forest fires and deforestation in the central Amazon: effects of landscape

and climate on spatial and temporal dynamics. **Journal of Environmental Management**, v.288, p.112310, 2021.

DOS SANTOS, A.C.; DA ROCHA MONTENEGRO, S.; FERREIRA, M.C.; BARRADAS, A.C.S.; SCHMIDT, I.B. Managing fires in a changing world: fuel and weather determine fire behavior and safety in the neotropical savannas. **Journal of Environmental Management**, v.289, p.112508, 2021.

DRISCOLL, D.A.; ARMENTERAS, D.; BENNETT, A.F.; BROTONS, L.; CLARKE, M.F.; DOHERTY, T.S.; HASLEM, A.; KELLY, L.T.; SATO, C.F.; SITTERS, H.; AQUILUÉ, N. How fire interacts with habitat loss and fragmentation. **Biological Reviews**, v.96, p.976-998, 2021.

ELITH, J.; PHILLIPS, S.J.; HASTIE, T.; DUDÍK, M.; CHEE, Y.E.; YATES, C.J. A statistical explanation of MaxEnt for ecologists. Diversity and Distributions, v.17, p.43-57, 2011.

FERREIRA, I.J.; CAMPANHARO, W.A.; BARBOSA, M.L.; SILVA, S.S.D.; SELAYA, G.; ARAGÃO, L.E.; ANDERSON, L.O. Assessment of fire hazard in Southwestern Amazon. Frontiers in Forests and Global Change, v.6, p.1107417, 2023.

FIDELIS, A.; SCHMIDT, I.B.; FURQUIM, F.F.; OVERBECK, G.E. Burning in the Pampa and Cerrado in Brazil. **Global Application of Prescribed Fire,** p.38, 2022.

FLORES, B.M.; MONTOYA, E.; SAKSCHEWSKI, B.; NASCIMENTO, N.; STAAL, A.; BETTS, R.A.; LEVIS, C.; LAPOLA, D.M.; ESQUÍVEL-MUELBERT, A.; JAKOVAC, C.; NOBRE, C.A. Critical transitions in the Amazon Forest system. **Nature**, v.626, p.555-564, 2024.

FONSECA, M.G., ANDERSON, L.O., ARAI, E., SHIMABUKURO, Y.E., XAUD, H.A., XAUD, M.R., MADANI, N., WAGNER, F.H. AND ARAGÃO, L.E. Climatic and anthropogenic drivers of northern Amazon fires during the 2015–2016 El Niño event. Ecological applications, v.27, p.2514-2527, 2017.

FONSECA, M.G., ALVES, L.M., AGUIAR, A.P.D., ARAI, E., ANDERSON, L.O., ROSAN, T.M., SHIMABUKURO, Y.E. AND DE ARAGÃO, L.E.O.E.C. Effects of climate and land-use change scenarios on fire probability during the 21st century in the Brazilian Amazon. Global change biology, v.25, p.2931-2946, 2019.

FORKEL, M., ANDELA, N., HARRISON, S.P., LASSLOP, G., VAN MARLE, M., CHUVIECO, E., DORIGO, W., FORREST, M., HANTSON, S., HEIL, A., LI, F. Emergent relationships with respect to burned area in global satellite observations and fire-enabled vegetation models. Biogeosciences. 2019 Jan 11;16(1):57-76.

FRIELER, K. et al. Scenario set-up and forcing data for impact model evaluation and impact attribution within the third round of the Inter-Sectoral Model Intercomparison Project (ISIMIP3a). EGUsphere 2023, 1–83 (2023).

GELMAN, ANDREW; CARLIN, JOHN B.; STERN, HAL S.; DUNSON, DAVID B.; VEHTARI, AKI; RUBIN, DONALD B. (2013). Bayesian Data Analysis, Third Edition. Chapman and Hall/CRC. ISBN 978-1-4398-4095-5.

GIGLIO, L., BOSCHETTI, L., ROY, D. P., HUMBER, M. L., AND JUSTICE, C. O. The Collection 6 MODIS burned area mapping algorithm and product, Remote Sens. Environ., 217, 72–85, 2018.

GÖLTAS, M.; AYBERK, H.; KÜCÜK, O. Forest fire occurrence modeling in Southwest Turkey using MaxEnt machine learning technique. **iForest-Biogeosciences and Forestry**, v.17, p.10, 2024.

HANTSON, S.; ARNETH, A.; HARRISON, S.P.; KELLEY, D.I.; PRENTICE, I.C.; RABIN, S.S.; ARCHIBALD, S.; MOUILLOT, F.; ARNOLD, S.R.; ARTAXO, P.; BACHELET, D. The status and challenge of global fire modelling. Biogeosciences, v.13, p.3359-75, 2016.

HANTSON, S., KELLEY, D. I., ARNETH, A., HARRISON, S. P., ARCHIBALD, S., BACHELET, D., FORREST, M., HICKLER,T., LASSLOP, G., LI, F., MANGEON, S., MELTON, J. R., NIERADZIK, L., RABIN, S. S., COLIN PRENTICE, I.,SHEEHAN, T., SITCH, S., TECKENTRUP, L., VOULGARAKIS, A. AND YUE, C.: Quantitative assessment of fireand vegetation properties in historical simulations with fire-enabled vegetation models from the FireModel Intercomparison Project, Geoscientific Model Development Discussions , 2020.

HARDESTY, J., MYERS, R. AND FULKS, W. 2005, January. Fire, ecosystems, and people: a preliminary assessment of fire as a global conservation issue. In The George Wright Forum (Vol. 22, No. 4, pp. 78-87). George Wright Society.

HAAS, O., PRENTICE, I.C., HARRISON, S.P. Global environmental controls on wildfire burnt area, size, and intensity. Environmental Research Letters,13;17(6):065004, 2022.

HESSELBARTH, M. H. K.; SCIAINI, M.; NOWOSAD, J.; HANSS, S.; GRAHAM, L. J.; HOLLISTER, J.; WITH, K. A.; PRIVÉ, F.; PROJECT NAYUKI; STRIMAS-MACKEY, M. **Landscape Metrics for Categorical Map Patterns**, 2024. Available at: https://cran.r-project.org/web/packages/landscapemetrics/landscapemetrics.pdf.

HOFFMAN, M.D.; GELMAN, A. The No-U-Turn sampler: adaptively setting path lengths in Hamiltonian Monte Carlo. **Journal of Machine Learning Research**, v.15, p.1593-623, 2014.

JAYNES, E.T. Information theory and statistical mechanics. Physical Review, v.106, p.620–630,1957.

JIMÉNEZ-VALVERDE, A. Insights into the area under the receiver operating characteristic curve (AUC) as a discrimination measure in species distribution modelling. **Global Ecology and Biogeography**, v.21, p.498-507, 2011.

JING, W.A.N., QI, G.J., JUN, M.A., REN, Y., RUI, W.A.N.G. AND MCKIRDY, S., 2020. Predicting the potential geographic distribution of Bactrocera bryoniae and Bactrocera neohumeralis (Diptera: Tephritidae) in China using MaxEnt ecological niche modeling. Journal of Integrative Agriculture, 19(8), pp.2072-2082.

KRAWCHUK, M. A.; MORITZ, M. A. Burning issues: statistical analyses of global fire data to inform assessments of environmental change. Environmetrics, v.25, p.472–481, 2014.

KELLEY, D.I., HARRISON, S.P. Enhanced Australian carbon sink despite increased wildfire during the 21st century. Environmental Research Letters, v.9, p.104015, 2014.

KELLEY, D.I.; BISTINAS, I.; WHITLEY, R.; BURTON, C.; MARTHEWS, T.R.; DONG, N. How contemporary bioclimatic and human controls change global fire regimes. **Nature Climate Change**, v.9, p.690-696, 2019.

KELLEY, D.I.; BURTON, C.; HUNTINGFORD, C.; BROWN, M.A.; WHITLEY, R.; DONG, N. Low meteorological influence found in 2019 Amazonia fires. **Biogeosciences Discussions**, p.1-17, 2021.

LAPLACE PS. Analytical probability theory. Courcier; 1820.

LI, B., LIU, B., GUO, K., LI, C. AND WANG, B., 2019. Application of a maximum entropy model for mineral prospectivity maps. Minerals, 9(9), p.556.

LI, S.; RIFAI, S.; ANDERSON, L. O.; SPARROW, S. Identifying local-scale meteorological conditions favorable to large fires in Brazil. **Climate Resilience and Sustainability**, v.1, e11, 2022.

LIBONATI, R.; GEIRINHAS, J.L.; SILVA, P.S.; MONTEIRO DOS SANTOS, D.; RODRIGUES, J.A.; RUSSO, A.; PERES, L.F.; NARCIZO, L.; GOMES, M.E.; RODRIGUES, A.P.; DACAMARA, C.C. Drought–heatwave nexus in Brazil and related impacts on health and fires: a comprehensive review. **Annals of the New York Academy of Sciences**, v.1517, p.44-62, 2022.

LIBONATI, R.; GEIRINHAS, J. L.; SILVA, P. S.; RUSSO, A.; RODRIGUES, J. A.; BELÉM, L.B.C.; NOGUEIRA, J.; ROQUE, F.O.; DACAMARA, C.C.; NUNES, A. M. B., MARENGO, J. A.; TRIGO, R. M. Assessing the role of compound drought and heatwave events on unprecedented 2020 wildfires in the Pantanal. **Environmental Research Letters**, v.17, p.015005, 2022b.

LOBO, J.M.; JIMÉNEZ-VALVERDE, A.; REAL, R. AUC: a misleading measure of the performance of predictive distribution models. **Global Ecology and Biogeography,** v.17, p.145-151, 2008.

MAPBIOMAS PROJECT. **Coleção 7 da série anual de mapas de cobertura e uso da terra do Brasil**. 2022. Available at: https://brasil.mapbiomas.org/downloads/.

MAPBIOMAS FOGO. Coleção 2 do mapeamento das cicatrizes de fogo do Brasil (1985-2022). 2023. Available at: https://brasil.mapbiomas.org/wp-content/uploads/sites/4/2023/08/ATBD_-_MapBiomas_Fogo_-_Colecao_2.pdf.

MATHISON C, BURKE E, HARTLEY AJ, KELLEY DI, BURTON C, ROBERTSON E, GEDNEY N, WILLIAMS K, WILTSHIRE A, ELLIS RJ, SELLAR AA. Description and evaluation of the JULES-ES set-up for ISIMIP2b. Geoscientific Model Development. 2023 Jul 27;16(14):4249-64.

MEIJER, J.R.; HUIJBREGTS, M.A.J.; SCHOTTEN, C.G.J.; SCHIPPER, A.M. Global patterns of current and future road infrastructure. **Environmental Research Letters**, v.13, e064006, 2018.

MENEZES, L.S.; DE OLIVEIRA, A.M.; SANTOS, F.L.; RUSSO, A.; DE SOUZA, R.A.; ROQUE, F.O.; LIBONATI, R. Lightning patterns in the Pantanal: untangling natural and anthropogenic-induced wildfires. Science of the Total Environment, v.820, p.153021, 2022.

MET OFFICE. **Iris: a powerful, format-agnostic, and community-driven Python package for analysing and visualising Earth science data, v3.6, 2010 – 2023**. Available at: http://scitools.org.uk/.

NOGUEIRA, J.M.; RAMBAL, S.; BARBOSA, J.P.R.; MOUILLOT, F. Spatial pattern of the seasonal drought/burned area relationship across Brazilian biomes: sensitivity to drought metrics and global remote-sensing fire products. **Climate**, v.5, p.42, 2017.

NUMATA, I.; SILVA, S.S.; COCHRANE, M.A.; D'OLIVEIRA, M.V. Fire and edge effects in a fragmented tropical forest landscape in the southwestern Amazon. **Forest Ecology and Management**, v.401, p.135-146, 2017.

OLIVEIRA, U.; SOARES-FILHO, B.; BUSTAMANTE, M.; GOMES, L.; OMETTO, J.P.; RAJÃO, R. Determinants of fire impact in the Brazilian biomes. **Frontiers in Forests and Global Change**, v.5, p.735017, 2022.

PENFIELD JUNIOR, P. Principle of maximum entropy: simple form. Massachusetts: Massachusetts Institute of Technology, 2003.

PETERSON, A.T.; SOBERON, J.; PEARSON, R.G.; ANDERSON, R.P.; MARTINEZ-MEYER, E.; NAKAMURA, M.; ARAUJO, M.B. **Ecological niches and geographic distributions.** Princeton: Princeton University Press, 2011.

PHILLIPS, S.J., ANDERSON, R.P. AND SCHAPIRE, R.E. Maximum entropy modeling of species geographic distributions. Ecological modelling, 190:231-259, 2006.

PHILLIPS, S.J.; DUDIK, M. Modeling of species distributions with Maxent: new extensions and a comprehensive evaluation. **Ecography**, v.31, p.161–175, 2008.

RABIN, S. S. ; MELTON, J. R. ; LASSLOP, G. ; BACHELET, D. ; FORREST, M. ; HANTSON, S. ; KAPLAN, J. O. ; LI, F. ; MANGEON, S. ; WARD, D. S. ; YUE, C. The Fire Modeling Intercomparison Project (FireMIP), phase 1: experimental and analytical protocols with detailed model descriptions. **Geoscientific Model Development**. v.10, p.1175-97, 2017.

RADOSAVLJEVIC, A.; ANDERSON, R.P. Making better Maxent models of species distributions: complexity, overfitting and evaluation. **Journal of Biogeography**, v.41, p.629–643, 2013.

ROSAN, T.M.; SITCH, S.; MERCADO, L.M.; HEINRICH, V.; FRIEDLINGSTEIN, P.; ARAGÃO, L.E. Fragmentation-driven divergent trends in burned area in Amazonia and Cerrado. **Frontiers in Forests and Global Change**, v.5, p.801408, 2022.

SILVA JUNIOR, C.H.; BUNA, A.T.; BEZERRA, D.S.; COSTA JR, O.S.; SANTOS, A.L.; BASSON, L.O.; SANTOS, A.L.; ALVARADO, S.T.; ALMEIDA, C.T.; FREIRE, A.T.; ROUSSEAU, G.X. Forest fragmentation and fires in the eastern Brazilian Amazon–Maranhão State, Brazil. Fire, v.5, p.77, 2022.

SILVEIRA, M.V., PETRI, C.A., BROGGIO, I.S., CHAGAS, G.O., MACUL, M.S., LEITE, C.C., FERRARI, E.M., AMIM, C.G., FREITAS, A.L., MOTTA, A.Z. AND CARVALHO, L.M., 2020. Drivers of fire anomalies in the Brazilian Amazon: Lessons learned from the 2019 fire crisis. Land, 9(12), p.516.

SILVEIRA, M.V.; SILVA-JUNIOR, C.H.; ANDERSON, L.O.; ARAGÃO, L.E. Amazon fires in the 21st century: the year of 2020 in evidence. **Global Ecology and Biogeography**, v.31, p.2026-2040, 2022.

SINGH, M.; HUANG, Z. Analysis of forest fire dynamics, distribution and main drivers in the Atlantic Forest. **Sustainability**, v.14, p.992, 2022.

SPEARMAN, C. The proof and measurement of association between two things. In: JENKINS, J.J.; PATERSON, D.G. (Ed.). **Studies in individual differences: the search for intelligence**. [S.l.]: Appleton Century Crofts, 1961. p.45-58.

UNITED NATIONS ENVIRONMENT PROGRAMME (UNEP). Spreading like wildfire: the rising threat of extraordinary landscape fires. 2022. Available at: https://www.unep.org/resources/report/spreading-wildfire-rising-threat-extraordinary-landscape-fires.

VOLKHOLZ, J.; LANGE, S.; GEIGER, T. ISIMIP3a population input data (v1.2). **ISIMIP Repository**.

WILTSHIRE AJ, BURKE EJ, CHADBURN SE, JONES CD, COX PM, DAVIES-BARNARD T, FRIEDLINGSTEIN P, HARPER AB, LIDDICOAT S, SITCH S, ZAEHLE S. JULES-CN: a coupled terrestrial carbon–nitrogen scheme (JULES vn5. 1). Geoscientific Model Development. 2021 Apr 27;14(4):2161-86.

1434 WU, Y., LI, S., XU, R., CHEN, G., YUE, X., YU, P., YE, T., WEN, B., COÊLHO, M.D.S.Z.S.,
1435 SALDIVA, P.H.N. AND GUO, Y., 2023. Wildfire-related PM2. 5 and health economic loss of
1436 mortality in Brazil. Environment International, 174, p.107906.

1437 ZACHARAKIS, I., TSIHRINTZIS, V.A. Environmental Forest fire danger rating systems and
1438 indices around the globe: a review. Land, v.12, p.194, 2023.

1439

1440
1441

1442
1443
1444

1445

1446